Clay mineralogy of bauxites and palaeosols in Istria formed during regional subaerial exposures of the Adriatic Carbonate Platform

Durn, Goran; Ottner, Franz; Mindszenty, Andrea; Tišljar, Josip; Mileusnić, Marta

Clay mineralogy of bauxites and palaeosols in Istria formed during regional subaerial exposures of the Adriatic Carbonate Platform

Goran DURN[1], Franz OTTNER[2], Andrea MINDSZENTY[3], Josip TIŠLJAR[1] and Marta MILEUSNIĆ[1]

This excursion is largely based upon the Field Trip P8 (Regional Subaerial Unconformities in Shallow-Marine Carbonate Sequences of Istria: Sedimentology, Mineralogy, Geochemistry and Micromorphology of Associated Bauxites, Palaeosols and Pedo-Sedimentary Complexes) of the 22nd IAS Regional Meeting held in Opatija, Croatia (DURN et al., 2003). Unlike the aforementioned field trip, this excursion comprises 3 stops instead of 8, but data on clays are presented in more detail.

1. INTRODUCTION AND GEOLOGICAL SETTING

The Istrian peninsula represents the NW part of the spacious Adriatic Carbonate Platform (for more details see VLAHOVIĆ et al., 2005). This part of the platform is composed of a succession of carbonate deposits more than 2000 m thick, of Middle Jurassic (Bathonian) to Eocene age, and is overlain by Palaeogene (Eocene) *Foraminiferal limestones*, *Transitional beds* (*Globigerina marls*) and flysch deposits (Fig. 1).

The most important geological structure of the Istrian peninsula is the Western Istrian Anticline (POLŠAK & ŠIKIĆ, 1973; MARINČIĆ & MATIČEC, 1991), as shown on Fig. 1.

According to VELIĆ et al. (1995a) carbonate and flysch deposits of Istria can be divided into four large-scale sequences. The 1st, 2nd and 3rd large-scale sequences are composed of carbonates, each terminated by important, long-lasting emersions, i.e. type 1 sequence boundaries (TIŠLJAR et al., 1998). They are divided into several laterally continuous units exhibiting gradual changes, typical of the facies diversity on carbonate platforms (Fig. 2).

The Jurassic and Lower Cretaceous deposits of Istria, ranging from the Bathonian to the Upper Albian (1st and 2nd large-scale sequences – Fig. 2), are characterized predominantly by shallow-marine deposition, only sporadically interrupted by periods of emersion (TIŠLJAR, 1978; TIŠLJAR et al., 1995; VELIĆ & TIŠLJAR, 1988; TIŠLJAR & VELIĆ, 1991; VELIĆ et al., 1995a, b). Limestones deposited in peritidal, tidal flat, tidal bar, and lagoonal to low-energy shallow marine environments predominate. Late-diagenetic dolomites only occur in the Upper Tithonian, Berriasian and Albian strata, whereas supratidal early-diagenetic dolomites are abundant in the Berriasian deposits. During the emersion phases breccia, clay and bauxite deposits were formed.

Recent investigations in Istria (VLAHOVIĆ et al., 1994; MATIČEC et al., 1996; TIŠLJAR et al., 1998), especially in its southern and northern parts, indicate the important role of synsedimentary tectonics which significantly modified the effects of eustatic sea-level fluctuations on this part of the Adriatic Carbonate Platform. In the Istrian part, these include the diachronism of the beginning of the regional Aptian–Early Albian emersion in Istria (Fig. 2): starting from the Late Barremian, Early or Late Aptian, distinct facies differentiation around the emerged parts, and contemporaneous transgression of deposits of different ages during the Middle Albian indicates the important influence of synsedimentary tectonics (VELIĆ et al., 1989), most probably expressed as low-amplitude folding (TIŠLJAR et al., 1995).

MATIČEC et al. (1996) presented new data on the age of the footwall of transgressive Palaeogene deposits in Istria (from Valanginian to Coniacian–Santonian). They reviewed the influence of Cretaceous synsedimentary tectonics, and also the palaeogeographic implications for the Istrian part of the Adriatic Carbonate Platform. For example, they pointed out that Late Cenomanian beds are the youngest Cretaceous deposits in northern Istria, which are karstified and covered by Eocene Foraminiferal limestones (column B on Fig. 2, after VLAHOVIĆ et al., 1994). In contrast, in southern Istria, sedimentation continued until the Upper Santonian (column A on Fig. 2, after TIŠLJAR et al., 1998), including the Late Cenomanian/Early Turonian eustatic sea-level rise which caused temporary drowning over a large part of the Adriatic Carbonate Platform (JENKYNS, 1991; GUŠIĆ & JELASKA, 1993; VLAHOVIĆ et al., 1994, 2002a), while in Central Istria there are localities where transgressive Palaeogene deposits overlie Lower Cretaceous limestones (MATIČEC et al., 1996).

Carbonate deposits of the Istrian Peninsula exhibit numerous exposure surfaces reflecting emergence. On this field trip, subaerial exposure surfaces associated with bauxites and palaeosols will be presented. Special attention will be given to clay mineralogy, sedimentology, geochemistry and the micromorphology of these materials. The following will be presented: (1) clayey bauxites associated with Kimmeridgian to Early Tithonian emergence, and

[1] *University of Zagreb, Faculty of Mining, Geology and Petroleum Engineering, Pierottijeva 6, HR-10000 Zagreb, Croatia (gdurn@rgn.hr)*
[2] *University of Natural Resources and Applied Life Sciences, Department of Applied Geology, Peter Jordan Strasse 70, A-1190 Vienna, Austria*
[3] *Eötvös Loránd University, Dept. of Applied & Environmental Geology, Pázmány Péter sétány 1/c, 1117 Budapest XI, Hungary*

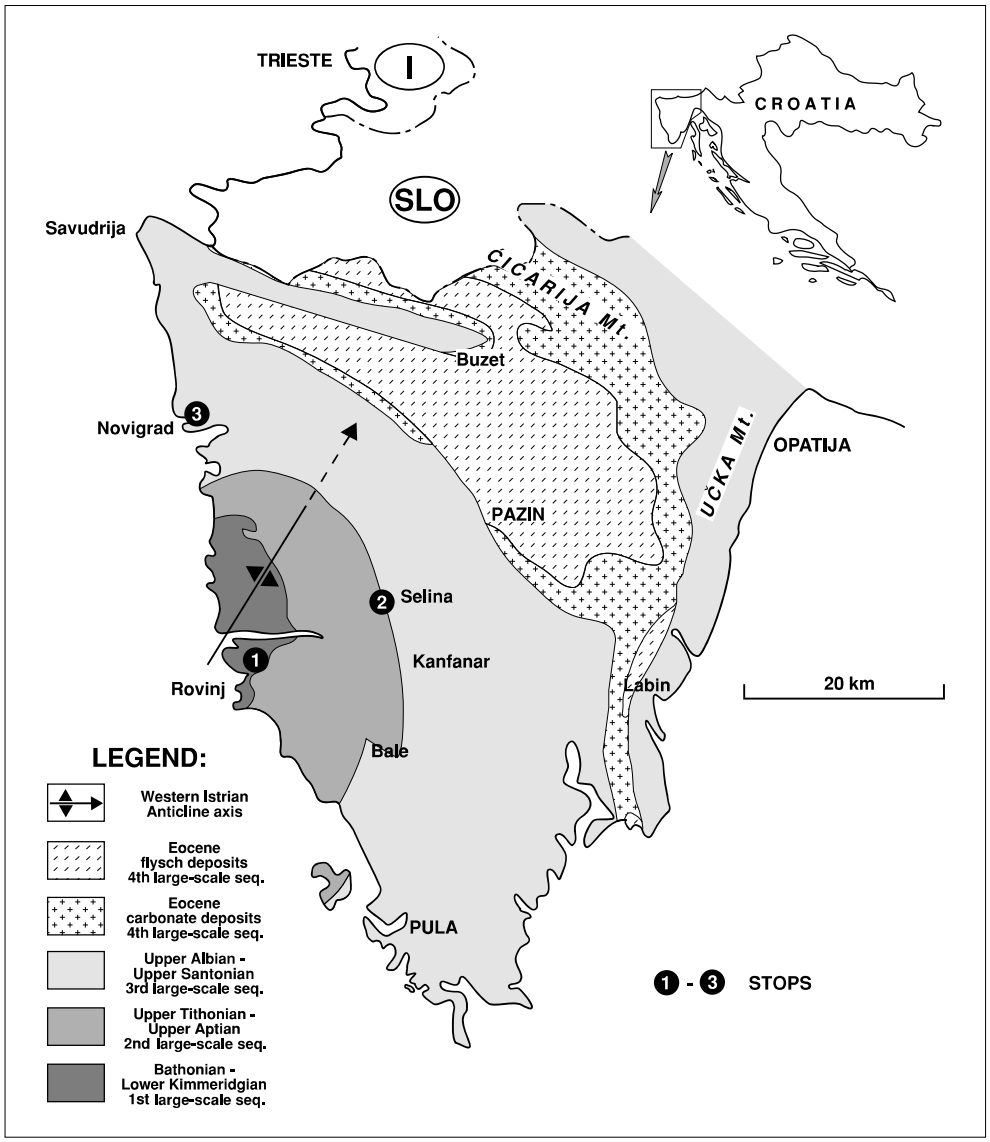

Fig. 1 Map showing the schematic distribution of large-scale sequences in Istria and location of the Western Istrian anticline (partly modified after VELIĆ et al., 1995a), with locations of the field trip stops.

(2) greenish–gray clays associated with Late Aptian–Late Albian regional emergence and relict polygenetic *terra rossa* soil.

2. JURASSIC BAUXITES

2.1. Introduction

Bauxites are humid tropical weathering products, similar to ferrallitic soils, the formation of which requires lengthy (>1 MY) subaerial exposure. The occurrence of bauxites is therefore generally considered as an indication of great periods of exposure and a hot humid climate. According to BÁRDOSSY & DERCOURT (1990), D'ARGENIO & MINDSZENTY (1991, 1992, 1995), MINDSZENTY & D'ARGENIO (1994) and COMBES & BÁRDOSSY (1994), subaerial exposure conducive to bauxitization is almost always the result of tectonically controlled uplift and the associated relative sea-level fall (which may or may not be coincident with a lower order eustatic event). As to the possible tectonic settings, three major cases are considered (D'ARGENIO & MINDSZENTY, 1995): (1) collisional settings, on the exposed/eroded tops of nappe-stacks or on flexural fore-bulges, (2) in passive plate interior settings affected by the change of intraplate stress, and (3) in strike-slip affected sectors at places of transpression-related uplift or on the tip of fault-bounded blocks (Fig. 3). In this excursion, one of three major settings will be presented: the Rovinj–1 bauxite deposit of Jurassic age is considered that of a passive plate interior under interplate stress (Type 2 sensu D'ARGENIO & MINDSZENTY, 1995).

2.2. Stop 1: Late Kimmeridgian–Early Tithonian emersion with bauxite deposit (Bauxite Pit near Rovinj, western Istria)

2.2.1. General framework

Although the likely palaeogeographic position of Istria in the Late Jurassic period was well within the inter-tropical belt (according to CHANNELL, 1996; STAMPFLI & MOSAR, 1999), the mechanism which resulted in the sufficiently lengthy exposure deserves attention, since it apparently counteracted the uniform thermal subsidence considered to be characteristic of most Jurassic Periadriatic carbonate platforms (e.g. BERNOULLI, 2001). The bauxitiferous unconformity of Rovinj, indicates that in the Kim-

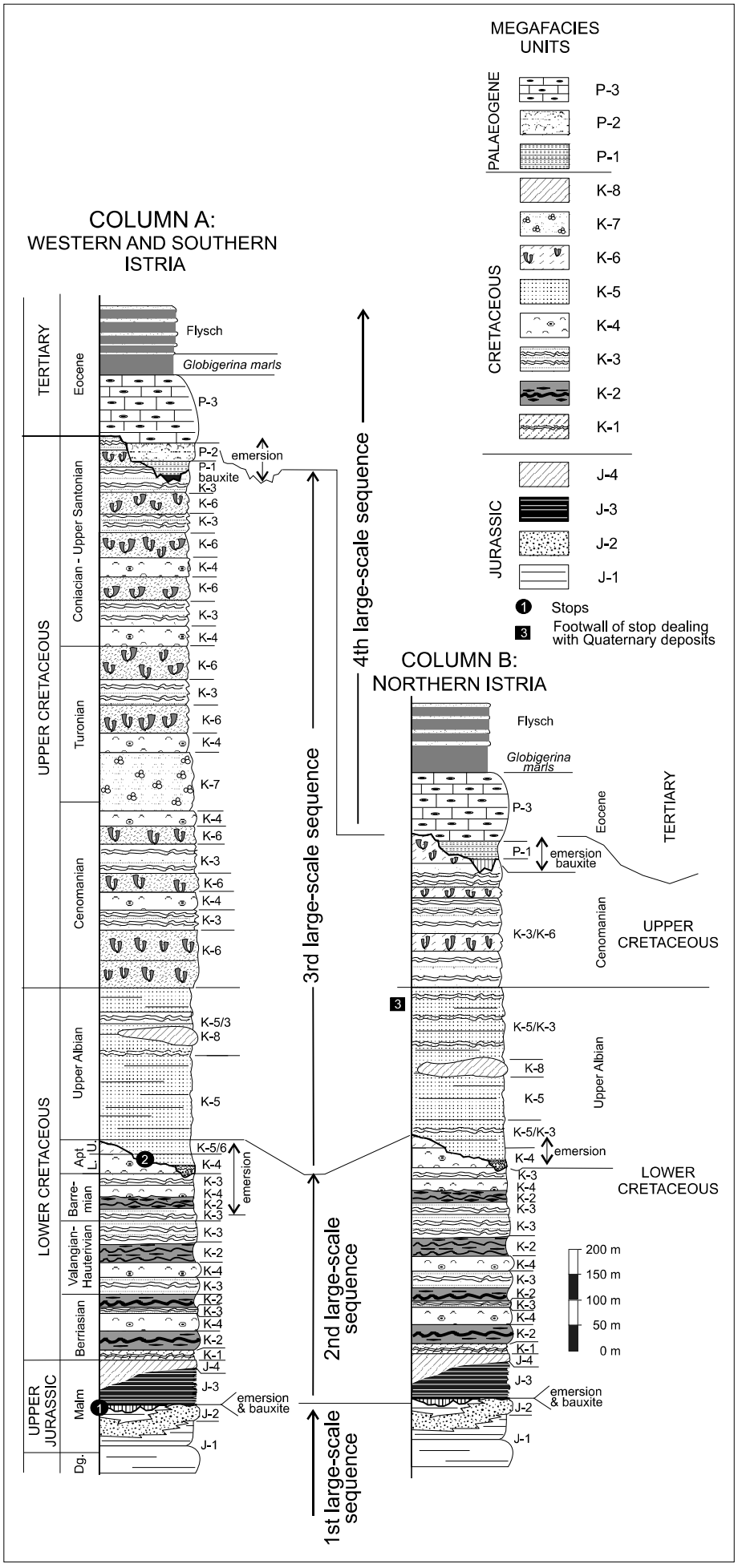

Fig. 2 Schematic geological columns of central and southern Istria (A) and northern Istria (B) showing four emersion-bound large-scale sequences with megafacies units and locations of the excursion stops (partly modified after TIŠLJAR at al., 1998, 2002). Legend of the megafacies units (after TIŠLJAR et al., 2002): Flysch deposits (in the lowermost part *Transition beds* or "*Globigerina marls*"; turbidites: alternation of carbonate sandstones and marls, in some places megabeds); P–2) *Foraminiferal limestones* (*Miliolidae- Alveolina-*, *Nummulites-* and *Discocyclina*-limestones, different environments: from the restricted inner part of the carbonate platform, through shallower and deeper parts of relatively open carbonate ramps to the upper slope); P–1) Liburnian deposits (fresh-water to brackish, and lagoonal – locally present, deposited in the lowermost parts of the palaeorelief); K–8) Late-diagenetic dolomites; K–7) Drowned platform limestones with pelagic fauna ("*calcisphera limestones*"); K–6) "*Rudist limestones*" (wackestones, packstones, floatstones/rudstones with rudist bioclasts, in some places rudist biostromes and/or lithosomes); K–5) Foreshore–shoreface peloidal and skeletal grainstones/packstones; K–4) Lagoonal and shallow subtidal carbonate mud-bearing limestones; K–3) Peritidal–tidal flat limestones (pelletal and skeletal wackestones/packstones, LLH-stromatolites, frequent shallowing-upward cycles); K–2) Peritidal and vadose limestones in alternation with emersion and black-pebble breccia and clay pockets; K–1) Alternation of early diagenetic and late diagenetic dolomites (shallowing-upward cycles consisting mostly of late-diagenetically dolomitised subtidal–intertidal deposits and supratidal early-diagenetic dolomites capped by fenestral stromatolites, desiccation cracks and erosion surfaces); J–4) Late-diagenetic dolomites (late diagenetic dolomitization of the limestones of megafacies unit J–3); J–3) Peritidal shallowing-upward cycles (consisting mostly of stylolitised mudstone and fenestral mudstone with erosion surfaces or desiccation cracks, frequently capped by storm-tide deposits with vadose diagenesis – "*Kirmenjak unit*"); J–2) Thick-bedded ooid grainstones and bioclastic rudstones (composed of ooids and bioclasts of bryozoans, corals, stromatoporoids and foraminifera – high-energy tidal-bar facies – "*Muča unit*"); J–1) Lagoonal and shallow subtidal pelletal and carbonate mud-bearing limestones ("*Lim unit*" and "*Monsena unit*").

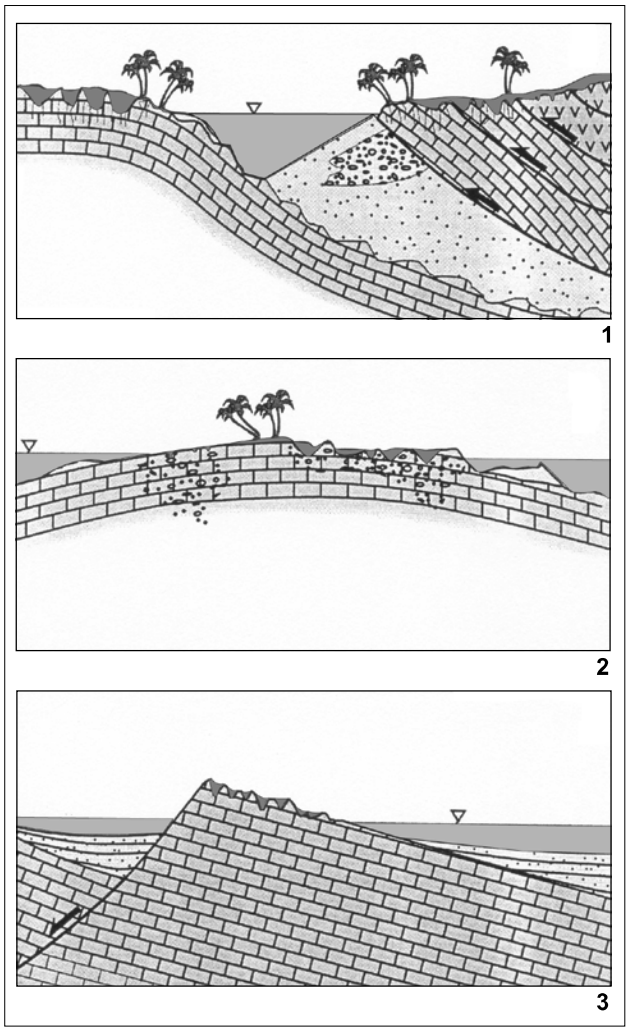

Fig. 3 Diagram showing three principal types of bauxites (after MINDSZENTY & D'ARGENIO, 1994). For explanation see text.

meridgian to the Tithonian, the subsidence of the Istrian part of the Adriatic Carbonate Platform domain was interrupted for some reason. Considering the Jurassic palaeoposition of Istria (e.g. on the palaeogeographic maps of DERCOURT et al. 1986; MANATSCHAL & BERNOULLI, 1998 or STAMPFLI & MOSAR, 1999), it is very likely that the tectonic setting of the Rovinj bauxite is that of a passive plate interior under intraplate stress (Type 2): on all three maps the Istrian peninsula plots close to the northern tip of, but still clearly within the Apulian Promontory (or Adria Microplate) (Fig. 4). Ongoing closure of the Vardar ocean along the distant eastern margins of the Apulian Promontory may have been responsible for intraplate stress generating gentle deformation in the Adriatic sector, resulting in exposure and bauxite formation. The associated relatively short stratigraphic gap (about 6 MY), lack of an appreciable angular unconformity between the bauxite, its bedrock and cover, and the fact that there is no abrupt facies change across the unconformity, (platform-type sedimentation continues apparently unchanged after the subaerial event) all reinforce the idea that the bauxite of Rovinj belongs to the aforementioned Type 2.

It should be noted that the Rovinj–1 deposit is not an isolated bauxite occurrence. According to BÁRDOSSY (1982), ŠINKOVEC & SAKAČ (1991), and others, in late Jurassic times, roughly contemporaneous bauxites, fossilized by Kimmeridgian to Tithonian shallow water carbonate sediments, occur at several localities within Greater Apulia (Fig. 5). From Greece through Montenegro to Slovenia (Amorgos, Parnass, Euboea, Viduša, Prokletije, Hrušica etc.), smaller or larger occurrences testify that this event of gentle deformation, though probably not strictly contemporaneous and of varying intensity, was of regional significance. Instead of having been restricted to the Adriatic sector, it also affected the Adriatic Carbonate Platform and seems to correlate very well with karst bauxite deposits as far south as the Hellenides or the attached shelf of the African craton (the bauxite of Mte Gallo/Sicliy – Di STEFANO et al., 2002).

2.2.2. Geological setting and sedimentological characteristics below and above the Late Kimmeridgian–Early Tithonian emersion surface in the Rovinj–1 bauxite deposit

At Stop 1 within the Rovinj–1 bauxite deposit we will see the end of the Late Kimmeridgian–Early Tithonian emersion bauxite deposit and the beginning of the Late Tithonian–Late Aptian large-scale sequence (2nd large-scale sequence on Figs. 2 and 6). The Bathonian–Early Kimmeridgian sequence is aproximately 200 m thick, and is characterized by shallowing- and coarsening-upward trends. It is terminated either by the Kimmeridgian–Early Tithonian emersion with bauxite deposits, or with erosion and emersion breccia. Carbonate deposits of this lengthy sequence are divided into three units (TIŠLJAR & VELIĆ, 1987; VELIĆ & TIŠLJAR, 1988): (1) "*Monsena unit*"; (2) "*Lim unit*" and (3) "*Muča unit*" (Fig. 6).

Monsena unit ("*Monsena micrites*") contains well-bedded foraminiferal wackestones to mudstones and fossiliferous wackestones, and rarely oncolite floatstones, deposited in the shallow subtidal lagoon and/or in restricted shallows. Debris of molluscs, hydrozoans and echinoderms drifted sporadically into environments where mud deposition predominated. The biofacies is characterized by benthic foraminiferal assemblages, which indicate a Bathonian age and, from the sequence of superposition, a Callovian age.

Lim unit (Oxfordian "*Lim pelletal limestones*") is composed of thick-bedded and massive fine-grained pelletal packstone/wackestones deposited in low-energy subtidal environments. On the basis of the fossil association these deposits are attributed to the lower parts of the Upper Jurassic, i.e. to the Oxfordian and Lower Kimmeridgian (*Salpingoporella* sellii zone).

Muča unit (Oxfordian "*Ooid and bioclastic limestones*") is the lateral counterpart of the *Lim unit*. The main lithofacies characteristic of the *Muča unit* is rhythmical alternation, i.e. cyclic deposition of three limestone types:

(a) *Peloidal and skeletal wackestones* deposited in a shallow subtidal environment under low energy conditions;

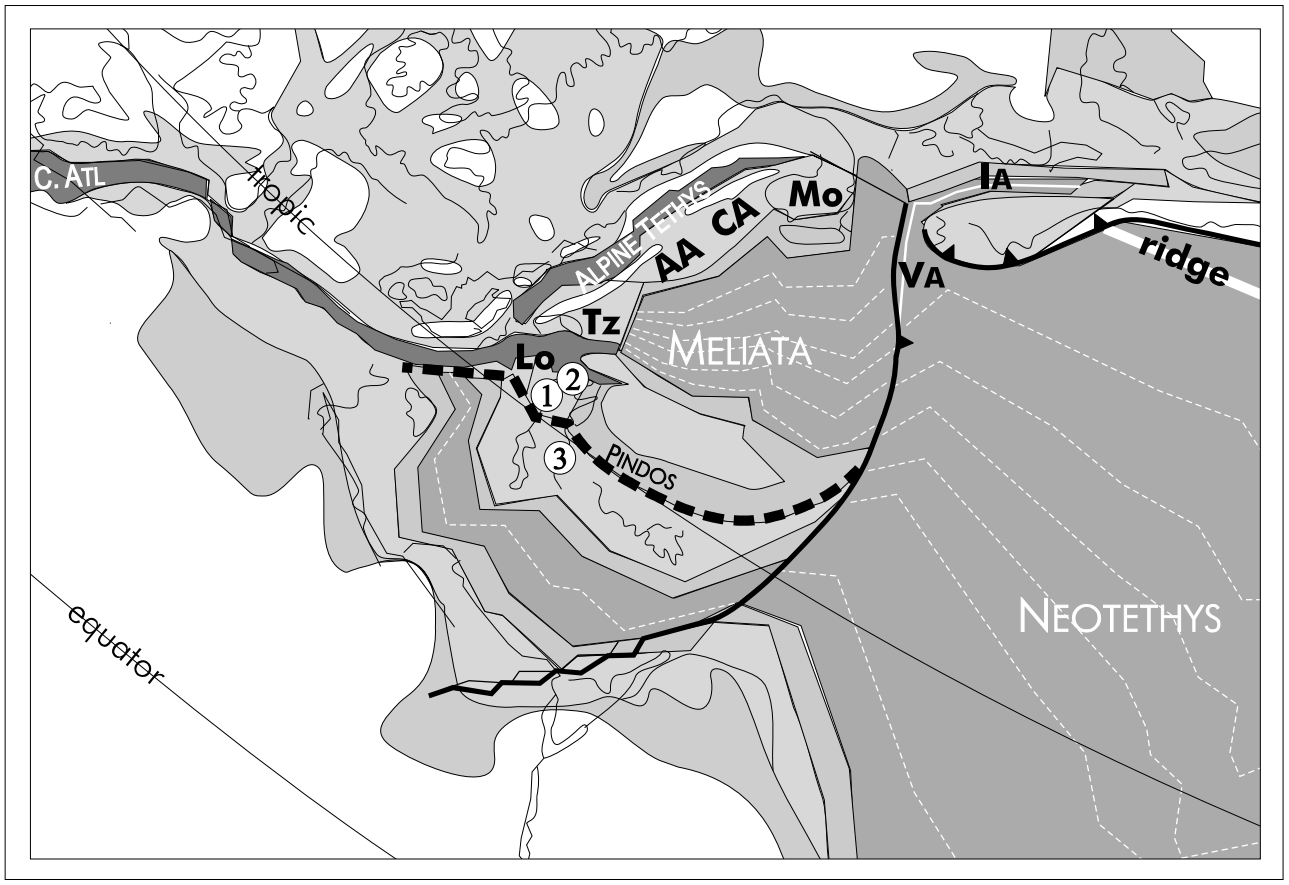

Fig. 4 The palaeographic map of the Sinemurian (after STAMPFLI & MOSAR, 1999), with the position of Jurassic bauxites in Istria (1), Slovenia (2) and Herzegovina and Montenegro (3). Locations of the bauxites after BARDOSSY & DERCOURT (1990), slightly modified.

(b) *Oolitic grainstones with cross-bedding* deposited on a tidal bar under a predominantly tidal influence, and

(c) *Thick-bedded oolitic grainstones and bioclastic rudstones* composed of coarse hydrozoans, corals, and mollusc bioclasts (cortoids), foraminiferal tests and *Cladocoropsis* and other stromatoporoid debris.

The biofacies of the *Muča unit* is characterized by different groups of organisms, especially in the *b* and *c* members. The most frequent components of the *c* member are reef-builders (corals, hydrozoans and other stromatoporoids), echinoderms, molluscs and foraminifera. Thickening-upward and coarsening-upward cycles were produced by migration of coarse-grained biodetritus. These deposits were produced by the disintegration of reefs during storm events and deposited in high-energy conditions in the form of prograding tidal-bar facies (TIŠLJAR & VELIĆ, 1987). On the basis of the fossil association these deposits are, like their lateral counterpart – *Lim unit* – attributed to the lower parts of the Upper Jurassic – to the Oxfordian and Lower Kimmeridgian.

Lowermost part of the *Kirmenjak unit* above the uderlying bauxite is characterized by an oscillating transgression (Figs. 6 and 7). It represents the first part of the second transgressive–regressive large-scale sequence of Jurassic–Cretaceous shallow-water carbonates of western and southern Istria (Figs. 2 and 6). The lower part of the ***Kirmenjak unit*** represents (after TIŠLJAR, 1986, and TIŠLJAR at al., 1995) shallowing-upward cycles composed of three members (Fig. 6):

(a) a thin, laterally variable bed of black-pebble breccia with carbonate, clayey or marly matrix. This member was formed by the redeposition of material originating from marsh deposits, enriched in organic matter, which was eroded and transported by storm activity over the black, supratidal and upper intertidal, oxygen-deficient, brackish and/or partly freshwater deposits, during a relative sea-level rise. They occur as fragments of intertidal or subtidal black-pebbles (breccia and conglomerates), partly in the form of tidal channel fills (TIŠLJAR, 1986);

(b) a thick-bedded (100 to 200 cm) stylolitized mudstone with rare bioclasts of *Clypeina jurassica* FAVRE, *Salpingoporella annulata* CAROZZI, and *Campbelliella striata* (CAROZZI). In some of the cycles the upper part is characterized by vertical bioturbation, fenestral fabric, desiccation cracks and erosion surfaces. This member was deposited in a low-energy subtidal to low intertidal environment;

(c) in this part of the *Kirmenjak unit* the third member is not always present (it is typical of the middle and upper parts of the unit); it is characterized by variable lithology and textures including vadose fabrics, intraclasts with pisoid coatings, and in places by brackish to freshwater(?) stromatolites. The upper bedding surfaces are sharp, irregular with desiccation cracks and/or erosion

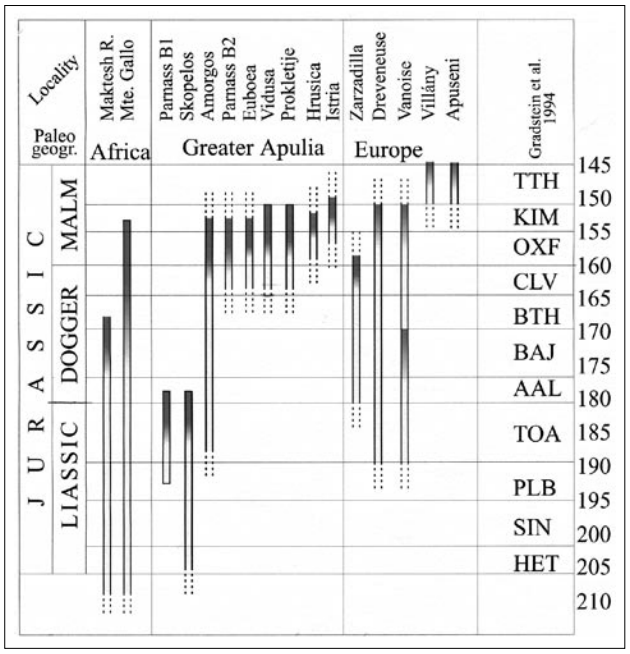

Fig. 5 Stratigraphic position of Jurassic bauxites. Data from BARDOSSY (1982), BARDOSSY & DERCOURT (1990), BORDEA & MANTEA (1991), COMBES (1990), Di STEFANO et al. (2002), DUDICH & MINDSZENTY (1984), ELLENBERGER (1955), FERLA & BOMMARITO (1988), MOLINA et al. (1991), NICHITTA (1988), ŠINKOVEC & SAKAČ (1991), SIMMONE et al. (1991), RADOJČIĆ (1982), TIŠLJAR et al. (1995), VERA et al. (1988).

features. This member was formed in an intertidal and/or vadose zone.

For more information on the palaeogeographical and sedimentological characteristics below and above the Kimmeridgian–Early Tithonian emersion surface in the western Istria see VLAHOVIĆ et al. (2003).

2.2.3. Bauxite and immediate cover

The Rovinj bauxite occurs at the contact of Upper Oxfordian–Lower Kimmeridgian and Upper Tithonian strata in an apparent stratigraphic gap of relatively short duration (about 6 MY) (Fig. 6). There is no noticeable angular unconformity associated with the erosion surface. According to TIŠLJAR et al. (1995, see Fig. 6), the subaerial phase is supposed to have lasted from the latest Oxfordian/earliest Kimmeridgian to the Middle Tithonian. Palaeokarstified thick-bedded ooid grainstones and bioclastic rudstones (*Muča unit*) are exposed in the bauxite pit, interrupted by the subaerial unconformity associated with bauxites. They are overlain by the *Kirmenjak unit* consisting of clay, breccia and mudstone followed by black-pebble breccia, stylolitized mudstone and fenestral mudstone.The uneven karstic surface of the bedrock contains medium-size (2.0 to 2.5 m high) sub-soil pinnacles exposed by mining activity. Closer examination of the bedrock reveals evidence of several superimposed phases of dissolution, brecciation and cementation.

The bauxite deposit is about 400 m long and 300 m wide and its thickness decreases gradually from 20 m to 0 m towards the margin of the deposit (ŠINKOVEC, 1974). The bauxite is red in colour, muddy (pelitomorphic) with occasional round grains, and small ooliths. On the outcrop scale it is massive and shows a characteristic nodular to spheroidal parting. Joint surfaces are coated by Mn-oxide and/or kaolinite. The quality of the ore is medium to poor. It is highly argillaceous; the alumina to silica ratio is just above 2.6, with alumina around 46% and silica above 15% (ŠINKOVEC, 1974). Major minerals are boehmite, kaolinite, haematite, anatase and minor chlorite. Extraclasts identified by ŠINKOVEC (1974) include rare zircon, tourmaline and apatite grains, which testify to the relative isolation of the depositional environment from the non-carbonatic surroundings. As a possible source material, the dissolution residue of the host carbonates, plus windblown dust is proposed by ŠINKOVEC & SAKAČ (1991), whereas VLAHOVIĆ et al. (2000) put forward the idea of an additional fine-grained volcanoclastic contribution.

The uppermost 20–30 cm of the bauxite is heavily altered: its colour is greenish–grey to yellowish–white with vertical to subvertical extensions penetrating the underlying deep red bauxite (Fig. 7). The alteration having affected the iron-minerals is clearly of a redox nature and is closely related to the environmental change associated with the deposition of the cover-beds. After the long subaerial period, when bauxite has accumulated and partly even passed the early stages of diagenesis under vadose meteoric conditions, relative sea-level rise induced an obvious hydrological change. Leaching throughflow must have effectively ceased, pores became saturated first by freshwater then by seawater, and, as a result of microbial destruction of organic matter, (living plants or plant-litter), all free oxygen was extracted from the pores. Ongoing plant destruction under stagnant, oxygen-poor conditions resulted in what soil scientists call "gleying" – the characteristic patchy iron-removal around roots and other plant residue. Later on, interaction with saline pore-waters may have resulted in the formation of fine-grained pyrite. Deferrified veins with traces of organic matter, observed at the top of the bauxite, are interpreted as an effect of root activity. Namely, they probably represent the remains of roots from the soil which may have developed on the top of bauxite in an already marshy/brackish environment.

2.2.3.1. The "blue hole" sequence

Above the altered bauxite the lowermost part of the cover records the establishment of a palustrine–lacustrine environment with greyish, organic-rich marl and brecciated limestone, characterized by a very restricted fauna, (mainly ostracods according to VLAHOVIĆ et al., 2000), and probably representing a freshwater pond, formed as the groundwater table was pushed upwards by seawater rising through karstic channels from below. According to VLAHOVIĆ (1999) in the wider surroundings of the quarry, this basal layer shows considerable facies diversity reflecting the dissected karst topography resulting from the preceding lengthy subaerial episode. An analogous situation was described in detail by CARANNANTE et al. (1994) from above Cretaceous bauxites of Southern Italy, where the change from freshwater to the eventual fully marine environment, with intervening schizohaline episodes was documented by faunal changes, sedimentary struc-

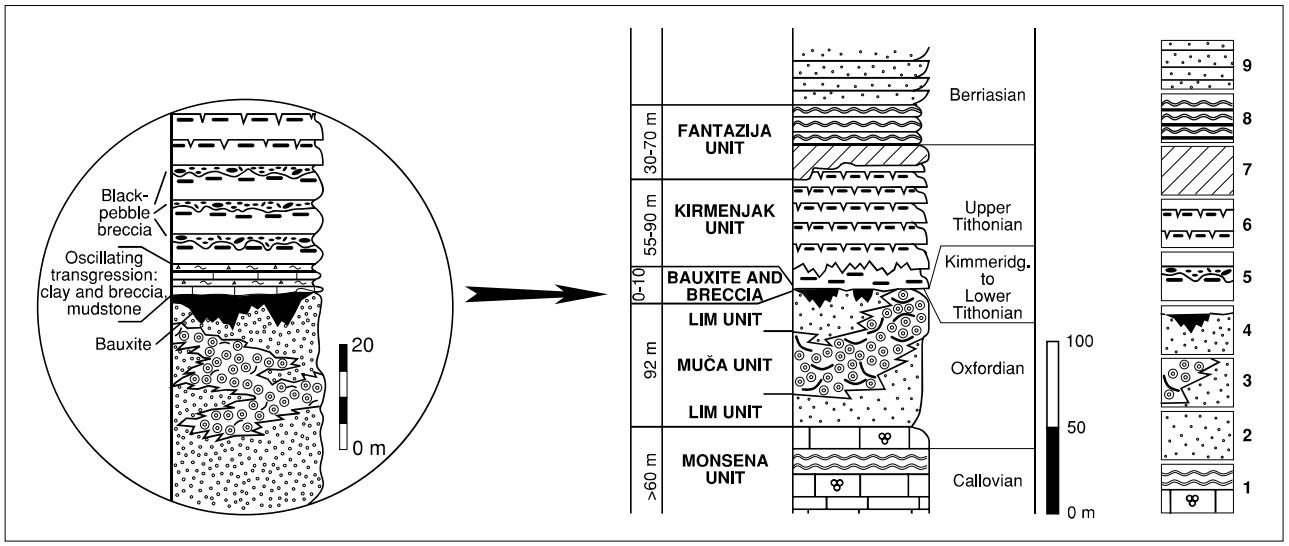

Fig. 6 Schematic geological column of Jurassic and older Lower Cretaceous deposits of western Istria with the location of stop 1 and details of emersions with bauxite deposits (after TIŠLJAR et al., 1994, partly modified according to lithostratigraphic units from VELIĆ & TIŠLJAR, 1988). Legend: 1) *Monsena unit*: well-bedded foraminiferal wackestone/mudstones (low-energy subtidal or lagoon); 2) *Lim unit*: thick-bedded and massive fine-grained pelletal packstone/wackestones (low-energy subtidal), with its lateral counterpart *Muča unit*; 3) *Muča unit:* thick-bedded ooid grainstones and bioclastic rudstones composed of ooids and bioclasts of bryozoans, corals, stromatoporoids and foraminifera (high-energy tidal-bar facies); 4) *Rovinj unit*: regressive breccia and bauxite (formed during a long-lasting emersion phase); 5) Lowermost part of the *Kirmenjak unit*: alternation of clay, breccia and mudstone (deposits of an oscillating transgression); 6) Lower part of the *Kirmenjak unit*: peritidal shallowing-upward cycles consisting mostly of black-pebble breccia, stylolitised mudstone and fenestral mudstone with erosion surfaces or desiccation cracks, frequently capped by storm-tide deposits with vadose diagenesis; 7) Late-diagenetic dolomites (= dolomitised limestones of the *Kirmenjak unit*); 8) *Fantazija dolomites*: shallowing-upward cycles consisting mostly of late-diagenetically dolomitised subtidal–intertidal deposits and supratidal early-diagenetic dolomites capped by fenestral stromatolites, desiccation cracks and erosion surfaces; 9) Berriasian shallowing-upward cycles consisting mostly of pelletal wackestones and *Favreina* packstone/grainstones and/or LLH stromatolites.

tures and diagenetic features. Based on the striking similarity with a Pleistocene/Holocene scenario described by RASMUSSEN & NEUMANN (1988) from the Bahamas, they compared the establishment of freshwater ponds on top of the bauxite-filled karst terrain to the establishment of the "blue holes" of the Bahamas and introduced the term "internal transgression" as opposed to "overland transgression". We have good reason to think that the lowermost part of the cover sequence of the Rovinj bauxite is another example of the filling of a karst relief from below, while higher up, shallowing-upward peritidal sequences and associated palaeosols show that after the initial "blue hole" stage, the sea encroached the whole platform, and normal marine conditions were again established.

2.2.3.2. Intercalations of green clay

Greenish–grey to yellow clay intercalations in the cover-beds may be signs of ephemeral exposure or, alternatively

Fig. 7 Bauxite deposit Rovinj–1. Contact of bauxite and first part of the second transgressive–regressive large-scale sequence of Jurassic–Cretaceous shallow-water carbonates.

represent clay influx from adjoining, slightly more highly elevated areas (still exposed when the depositional environment was already inundated).

When occurring at the top of shallowing-upward cycles and displaying associated dissolution phenomena, they are claimed to be signs of ephemeral exposure. It is worth noticing that the distribution of cm-sized palaeokarstic cavities seems to have been controlled by the pre-existing burrows of benthic organisms (or alternatively by roots of aquatic plants) having affected the muddy sediment while it was still soft. Differential hardening on exposure has fossilized these structures, which later became filled by clay washed in from the thin argillaceous soil blanket above, and cemented by calcite during the later stages of burial. Embedded in the green clay, corroded limestone fragments (occasionally also black pebbles) are interpreted as a dissolution breccia accumulated on the exposed surface.

When clay intercalations occur without accompanying palaeokarst features, they were possibly introduced to the depositional environment from external sources. The most plausible source would be the redeposited material of the bauxitic blanket covering adjoining slightly more highly elevated (and therefore not yet inundated) areas. Though no detailed mineralogical data on this material are available as yet, it is highly possible that early diagenesis in the lagoonal submarine environment would have substantially altered the bauxitic clay.

2.2.3.3. Chemical and mineralogical composition of bauxite and the lowermost part of the immediate cover

For the purpose of this fieldtrip, seven samples for chemical and mineralogical analyses were taken along a profile situated in the uppermost part of the bauxite and the lowermost part of the immediate cover (Fig. 8, Table 1). The uppermost sample analysed is situated 90 cm above the grey bauxite and represents a greenish–grey clay. Immediately above this sample there is a coarse brecciated zone, infilled with greenish–grey clay which probably represents a dissolution breccia accumulated on the exposed surface.

The chemical analyses were performed after $LiBO_2$ fusion with ICP–ES (major elements) and ICP–MS (trace elements). REE were analysed with ICP–MS. A semi-quantitative mineral composition was calculated from XRD, TG, FTIR and ICP–ES data.

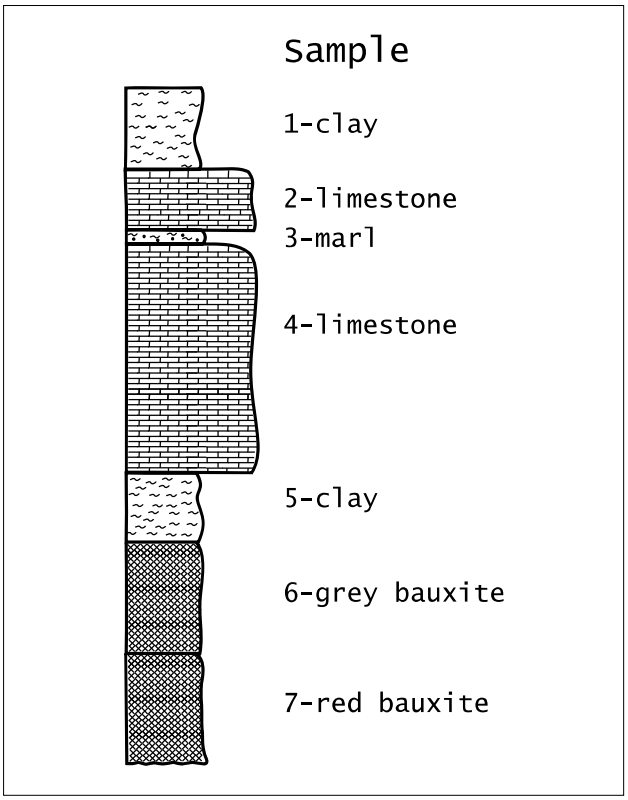

Fig. 8 Bauxite deposit Rovinj–1. Profile situated in the uppermost part of the bauxite and the lowermost part of the immediate cover.

2.2.3.3.1. Bauxite

The dominant mineral phases in both red and grey bauxite are kaolinite and boehmite (Table 2). The main iron-bearing phase in red bauxite is haematite and in grey bauxite pyrite. Both bauxites also contain chlorite and mixed-layer chlorite/vermiculite/illite (Tables 2 and 3). Compared to the red bauxite, grey bauxite is depleted in iron and arsenic, and, at the same time, enriched in sulphur (Table 4), and slightly enriched in cobalt, copper, zinc and lead (Table 5), i.e. in elements which have a general tendency to accumulate under reducing conditions. The mineralogy of the iron-bearing phases and the chemical composition, clearly indicates that red bauxites were deposited under oxidizing conditions (*vadose bauxites*), while grey bauxite (at the top of red bauxite), formed in a reducing environment as a result of hydrological change due to deposition of the coverbeds. Consequently, grey bauxite at the top of a

Sample	Description	Thickness	Munsell colour
1	clay	20 cm	greenish grey (6/1 for glay 1)
2	limestone (ostracod wackestone)	15 cm	–
3	marl	3 cm	yellow (2.5Y 7/6)
4	limestone (pyritized peloid--ostracod packstone)	55 cm	–
5	clay	17 cm	yellow (10YR 7/8)
6	grey bauxite	28 cm	greenish grey (6/1 for glay 1)
7	red bauxite	>800 cm	weak red red (10R 4/4)

Table 1 Bauxite deposit Rovinj–1. Description of profile situated in the uppermost part of the bauxite and lowermost part of the immediate cover.

	Kaolinite	Boehmite	Goethite	Haematite	Pyrite	Calcite	Other clay minerals
1	50	–	–	–	7	–	43
2	n.a.	n.a.	n.a.	n.a.	n.a.	n.a.	n.a.
3	20	–	4	–	–	40	36
4	n.a.	n.a.	n.a.	n.a.	n.a.	n.a.	n.a.
5	46	5	8	–	–	–	41
6	40	38	–	–	6	–	16
7	34	37	–	18	–	–	11

Table 2 Semiquantitative mineral composition of bauxites, clays and marl. Legend: n.a.) not analysed. For sample description see Table 1.

	Kaolinite	Illitic material	Mixed layer chlorite/ vermiculite/illite	Chlorite
1	+++	traces	++	++
2	n.a.	n.a.	n.a.	n.a.
3	++	++	+	+
4	n.a.	n.a.	n.a.	n.a.
5	+++	traces	++	++
6	++	–	+	+
7	++	–	+	+

Table 3 Clay mineral composition of the <2 μm fraction of bauxites, clays and marl. Legend: +++) dominant; ++) abundant ; +) minor; n.a.) not analysed. For sample description see Table 1.

red one can be considered *phreatic bauxite*. This is also supported by the distribution of REE (Figs. 9 and 10). The total REE content is 376.35 ppm in red and 261.76 ppm in grey bauxite. The $(La/Yb)_{ch}$ ratio in grey bauxite (6.36) is lower than that in red bauxite (8.50), and significantly lower than that of ES indicating HREE enrichment relative to LREE. Enrichment of HREE in grey bauxite is the result of the higher mobility of LREE in acidic reducing conditions.

Since chlorite is present in similar amounts in red and grey bauxite, its origin cannot be related solely to the reducing processes which affected the top of the red bauxite and converted it to grey bauxite, but also to burial diagenesis. It is interesting to note that ŠINKOVEC (1974) observed that the appearance of chlorite in both red and grey bauxite is similar. For more about chlorite and mixed-layer chlorite/vermiculite/illite, which was also detected in both bauxites, see the next section.

2.2.3.3.2. Lowermost part of the immediate cover

The immediate cover of grey bauxite is yellow clay (Fig. 8 and Table 1) which can be traced as a layer of variable thickness (up to 30 cm) within the area of the whole de-

	SiO_2 %	Al_2O_3 %	Fe_2O_3 %	MgO %	CaO %	Na_2O %	K_2O %	TiO_2 %	P_2O_5 %	MnO %	LOI %	TOTS %
1	40.15	29.89	6.08	1.89	1.09	0.09	2.43	1.54	0.02	0.02	16.6	3.70
2	n.a.	n.a.	n.a.	n.a.	n.a.	n.a.	n.a.	n.a.	n.a.	n.a.	n.a.	n.a.
3	26.24	15.99	4.98	1.97	21.76	0.04	2.66	0.79	0.02	0.07	25.2	0.06
4	n.a.	n.a.	n.a.	n.a.	n.a.	n.a.	n.a.	n.a.	n.a.	n.a.	n.a.	n.a.
5	37.20	32.18	8.04	2.08	0.62	0.09	1.81	1.50	0.04	0.02	15.9	0.09
6	22.58	50.15	5.55	0.66	0.12	0.06	0.30	2.42	0.03	0.06	17.9	3.38
7	18.87	46.89	18.22	0.60	0.16	0.05	0.25	2.20	0.04	0.14	12.3	0.07

Table 4 Chemical composition (major elements) of bauxites, clays and marl (in wt.%). Legend: n.a.) not analysed; TOTS) total sulphur. For sample description see Table 1.

	Co ppm	U ppm	Ba ppm	Ni ppm	Cu ppm	Pb ppm	Zn ppm	As ppm
1	36.4	27.0	169	146	24.8	23.3	145	14.5
2	n.a.	n.a.	n.a.	n.a.	n.a.	n.a.	n.a.	n.a.
3	78.8	9.1	108	99	18.4	21.7	153	41.0
4	n.a.	n.a.	n.a.	n.a.	n.a.	n.a.	n.a.	n.a.
5	283.0	4.9	129	315	222.9	223.3	714	34.7
6	136.5	6.9	46	244	15.3	124.3	107	1.2
7	27.6	5.3	47	205	6.2	72.5	96	5.6

Table 5 Chemical composition (trace elements) of bauxites, clays and marl (in ppm). Legend: n.a.) not analysed. For sample description see Table 1.

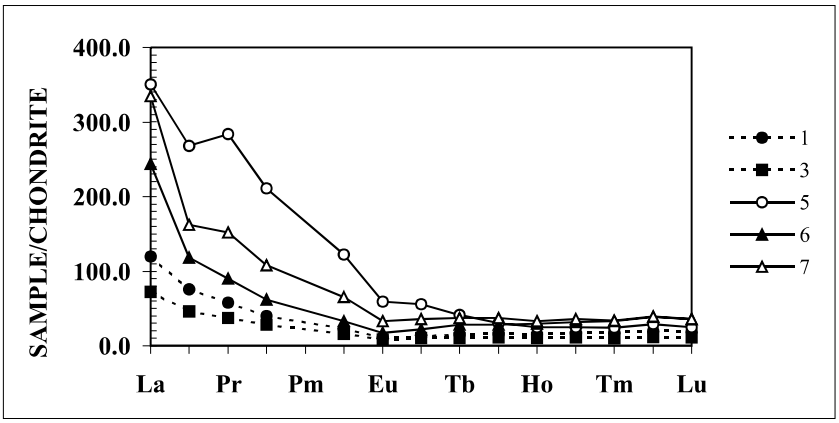

Fig. 9 Chondrite-normalized REE patterns of bauxites, clays and marl.

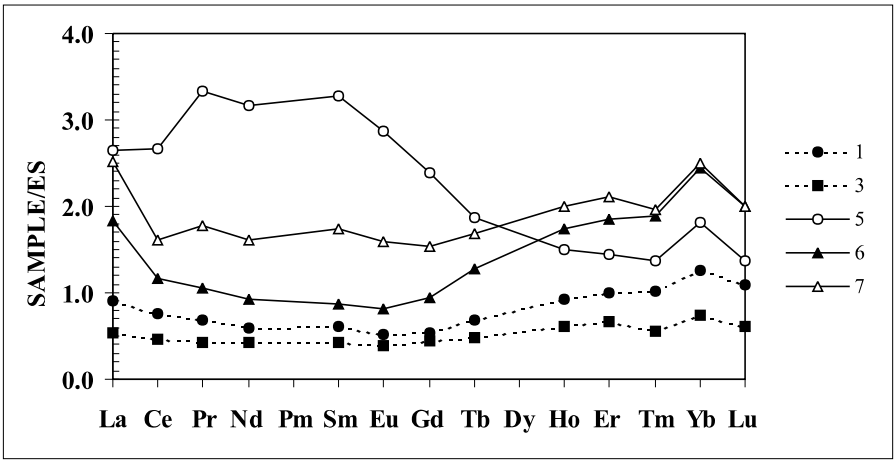

Fig. 10 European shale-normalized REE patterns of bauxites, clays and marl.

posit. The interesting point is its predominantly kaolinitic composition with boehmite as a minor phase (Table 2). The clay fraction is dominated by kaolinite, while chlorite and mixed-layer chlorite/vermiculite/illite are present in similar amounts as subordinate phases, and illitic material as traces (Table 3). This clay is especially enriched in Co, Ba, Ni, Cu, Pb, Zn, As (Table 5) and REE (the total REE content is 555.48 ppm). The chondrite normalized patterns and especially ES normalized patterns show that this clay is enriched in LREE and MREE, which can be an indication of repeated cycles of oxidation and reduction (Figs. 9 and 10). We tentatively propose that this clay represents redeposited material introduced to the depositional environment from the kaolinitic and bauxitic blanket covering adjoining slightly higher elevated areas. This clay is overlain by pyritized peloid/ostracod packstone and marl (Fig. 8, Table 1), which probably formed in a freshwater pond. The main mineral phase in marl is calcite (Table 2), while the clay fraction is dominated by illitic material and kaolinite, but chlorite and mixed-layer chlorite/vermiculite/illite are present in similar amounts as minor phases (Table 3). A high potassium content (Table 4), and, consequently, a high content of illitic material in this marl may be interpreted in two ways: either the external source of material supply altered (higher potassium input; e.g. K-feldspar, mica, illite), or weathering trends on land changed from *sialitization* (formation of kaolinite) and *allitization* (formation of Al-hydroxides) to *bisialitization* (formation of 2:1 clay minerals), as a consequence of climate change. A low value for the $(La/Yb)_{ch}$ ratio in the marl (6.16) indicates HREE enrichment relative to LREE (Fig. 10) and may suggest formation under acidic and reducing conditions. The marl is overlain by an ostracod-bearing wackestone, which, in turn, is covered with greenish–grey kaolinitic clay containing pyrite (Fig. 8, Tables 1 and 2). Immediately above this clay there follows a coarse brecciated zone infilled with greenish–grey clay, which probably represents a dissolution breccia accumulated on the exposed surface.

The clay fraction is dominated by kaolinite, while chlorite and mixed-layer chlorite/vermiculite/illite are present in similar amounts as subordinate phases and illitic material as traces, i.e. the clay mineral composition is very similar to that of the clay overlying the grey bauxite (Table 3). The colour of the clay and the presence of pyrite framboids may imply that this clay was affected by hydromorphic pedogenic processes related to ephermal exposure and represents a kind of a marshy soil. This is supported by its high U content (Table 5) and low $(La/Yb)_{ch}$ ratio (6.07). The mineralogical and chemical data support the "blue-hole" sequence story.

A few more words concerning the mineralogy of the clay fraction of the analysed samples.

Kaolinite

According to FTIR measurements it shows most properties of a poorly crystallized kaolinite (almost no absorption around 3670 ny). This is consistent with very low dehydroxylation temperatures (~550°C) and a low exothermal

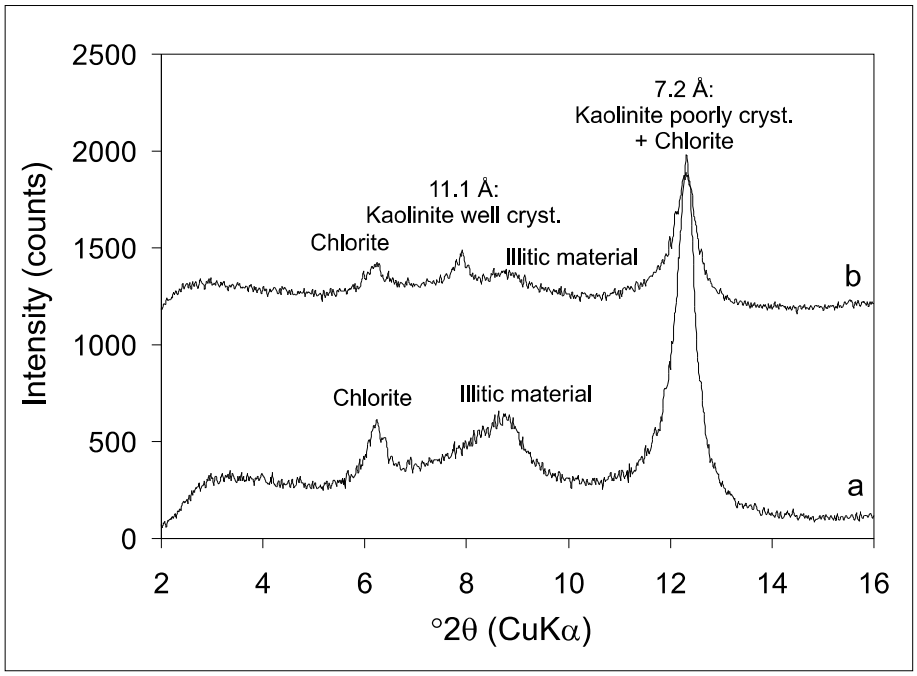

Fig. 11 Characteristic parts of XRD patterns of clay sample 1 (<2 µm fraction): (a) air dried; (b) K-saturated and DMSO-solvated.

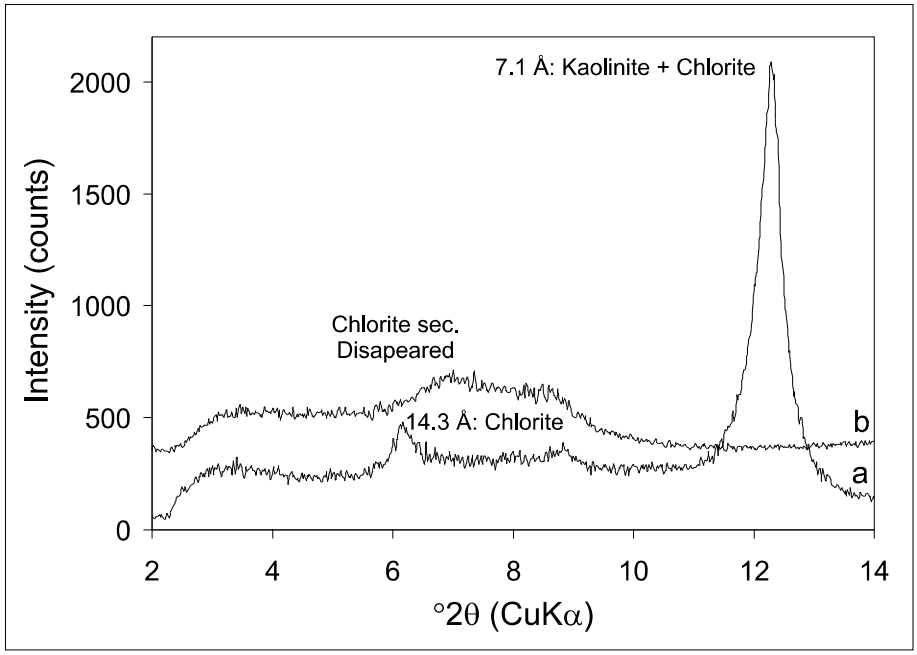

Fig. 12 Characteristic parts of XRD patterns of clay sample 5 (<2 µm fraction): (a) air dried; (b) Heated for one hour at 550°C.

reaction (950°C) in thermoanalysis. After treatment with DMSO and measurement by XRD, different amounts of well-crystallized kaolinite react by swelling (10 to 50%), but the rest of the kaolinite does not react, which means that it is poorly crystallized (Fig. 11).

Chlorite

All samples contain various amounts of chlorite, the highest content being observed in clays (samples 1 and 5). The very strong 003 reflexion (~4.77 Å) is noticable which is typical for Al-rich chlorites, e.g. *sudoite*. The second important fact is that chlorite is not stable against heating to 550°C (Fig. 12), which is typical for secondary chlorites (formed in moderately acidic environment).

Mixed-layer mineral

This is more or less present in all samples, particularly in clays (samples 1 and 5). However, our investigations of this mixed-layer mineral are far from being complete. Namely, we tentatively interpret this mineral as mixed-layer chlorite/vermiculite/illite because it must consist of at least 3 components:

1) *Vermiculite*: because it contracts after treatment with K to 10 Å, and we know from the thermoanalysis that high amounts of interlayer water are present in the range between 100 and 200°C, which is typical for smectites and vermiculites. The presence of vermiculite in the mixed-layer mineral is also obvious from comparison of K and Mg treated samples (Fig. 13). After treatment with K the

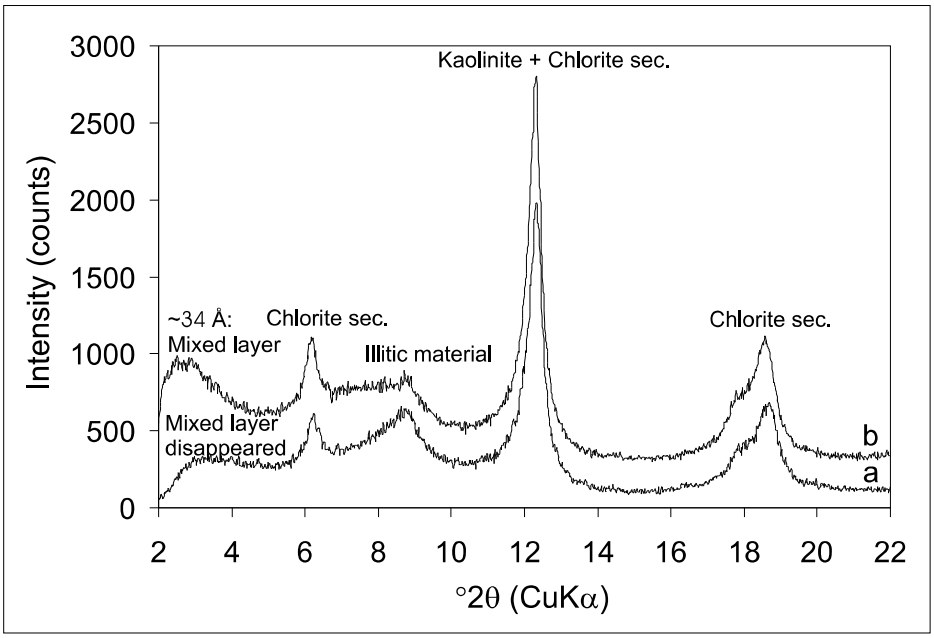

Fig. 13 Characteristic parts of XRD patterns of clay sample 1 (<2 μm fraction): (a) K-saturated; (b) Mg-saturated.

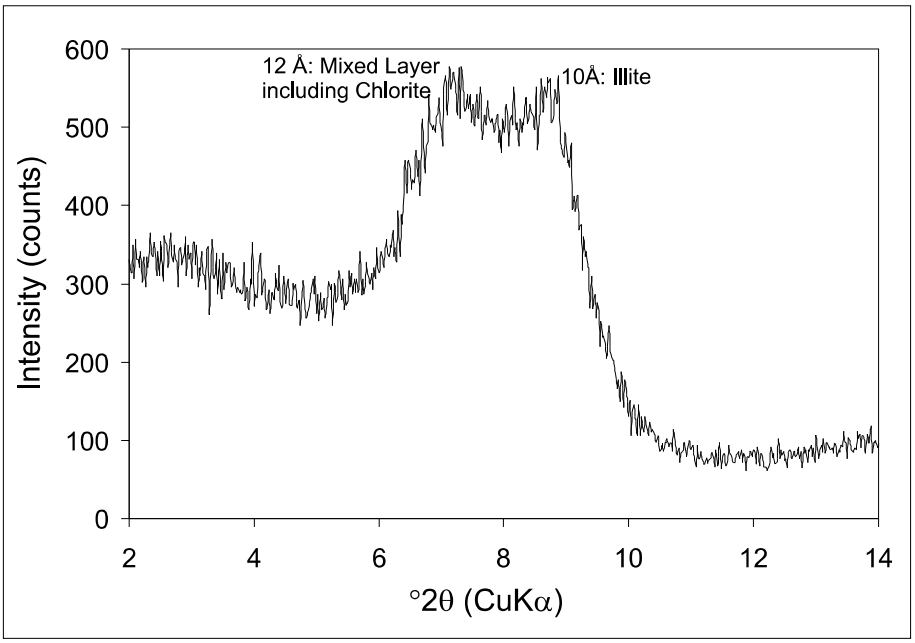

Fig. 14 Characteristic parts of XRD pattern of clay sample 1 (<2 μm fraction) heated for one hour at 550°C.

10 Å peak is much sharper (contraction of vermiculite in the mixed-layer mineral). Also, the change in the 34 Å area is caused by the vermiculite component in the mixed-layer mineral.

2) *Chlorite*: after heating to 550°C a very strong reflection appears around 12 Å, which is very typical of the 002 reflection of mixed-layer minerals containing chlorite (Fig. 14).

3) *Illitic material*: we know that K is present in relatively high amounts, no K bearing mineral other than illitic material is detected, and therefore it must occur in this mixed-layer mineral.

3. REGIONAL MIDDLE/LATE APTIAN–LATE ALBIAN EMERSION IN CENTRAL ISTRIA

3.1. General geological setting and sedimentological characteristics of the central Istrian area

At the beginning of the Aptian in the Istrian part of the Adriatic Carbonate Platform, spacious low-energy shallows and large lagoons were formed, where extensive amounts of fine carbonate detritus were deposited. The first 2–5 metres of the succession are commonly characterized by variable amounts of requieniid shells, mostly of *Toucasia* sp., and different benthic foraminifera, as well as numerous relatively large (1–8 cm) oncoids, with *Bacinella irregularis* RADOIČIĆ or gastropod shells as nuclei (=lower part of *Istarski žuti* zone).

The *Istarski žuti* zone of Lower Aptian age is characterized by rhythmic alternations of mudstone and *Bacinella-*

oncolites (i.e. oncoid floatstones), and it is yellow in colour (*Istarski žuti* = Istrian Yellow). It is subdivided into short and long rhythms (TIŠLJAR, 1978). *Short rhythms* are 25–50 cm thick, composed of layers of mudstone with rare oncoids and layers of oncolites. *Long rhythms* are 150–280 cm thick, composed of thick micrite beds (higher sedimentation rate) and a few short rhythms (lower sedimentation rate).

Bacinella-oncoids, which are typical components of the Lower Aptian limestones throughout the Dinarides, are always irregular in shape, and relatively large (mostly 5–80 mm), and are therefore sometimes referred to as "macroids". They have encrusted *Bacinella* skeletons in the central part, surrounded by a thinner or thicker oncoid envelope. Oncoids usually comprise 40–80 vol.% of the rocks, and in some parts, where they form oncoid crusts like hardgrounds, they are practically the only rock constituents (TIŠLJAR, 1983).

Mudstones were deposited during periods of higher accumulation rates, while in periods of low accumulation rates oncoids were formed, and deposits were intensely bioturbated. The entire unit was characterized by deposition in relatively deeper environments, resulting in relative accumulation rates approximately three times lower than the average for Lower Cretaceous deposits in Istria (VLAHOVIĆ, 1999). Those deeper environments were sporadically connected with the open sea.

The thickness of the Lower Aptian oncolitic limestones is very variable, as a consequence of differences in the beginning and duration of the regional Middle/Late Aptian–Late Albian emersion on the Istrian part of the Adriatic Carbonate Platform (VELIĆ et al., 1989). Namely, the duration of the emersion phase was variable, from 11–19 MY, depending upon the palaeogeographical position of the different localities. This was caused by differential amounts of synsedimentary tectonics modifying the eustatic signal, resulting in variable levels of relative sea-level fall, erosion and karstification during the Late Aptian and Early Albian (VELIĆ et al., 1989; TIŠLJAR et al., 1995; MATIČEC et al., 1996). For example, in the area of Seline (Stop 2) and Bale, emersion started during the Middle Aptian, while in the area of Kanfanar, emersion began during the Late Aptian. Exposure-related features are represented by greenish–grey clays, mainly in palaeokarst pits and coarse brecciated regolith. Clays associated with this emersion range in thickness from several centimetres up to 1 metre. Transitional zones between the shallow-water carbonates and emergent parts of the platform were characterized by either clay and marl deposition, or extensive coastal marshes with reducing conditions and deposition of black sediments (black-pebbles) enriched in plant remains and pyrite formed by sulphate-reducing bacteria (TIŠLJAR et al., 1995). A specific characteristic of the succession in the Tri jezerca (Stop 2), Kanfanar and Bale quarries is the abundant occurrence of blackened peritidal deposits as a consequence of reducing swamp conditions.

The beginning of Late Albian deposition is characterized by an oscillating transgression, and deposition of peritidal limestones and high-energy conglomerates (TIŠLJAR et al., 1995). Within these sediments, features indicating 3 to 6 short emersions, represented mainly by coarse brecciated zones, infilled with greenish–grey and greenish–yellow clays can be observed. This oscillatory transgression gradually covered the entire Istrian area at the beginning of the Late Albian, marking the beginning of deposition of a new large-scale sequence (Fig. 2), which lasted in southern Istria until the Late Santonian (column A on Fig. 2), and in northern Istria (column B on Fig. 2) until the Late Cenomanian (VELIĆ et al., 1995a; TIŠLJAR et al., 1995).

3.2. Stop 2: Middle Aptian–Late Albian emersion phase in the Tri jezerca quarry (near Selina village, central Istria)

In the Tri jezerca quarry, near Selina village (Figs. 4 and 15), building-stone known under the name of *Istarski žuti* (Istrian Yellow) was exploited. This stone is presently exploited in a few quarries in central Istria by the "Kamen Pazin" company. It is part of the Lower Aptian massive limestones, forming the uppermost part of the second large-scale sequence over a predominant area of Istria (Fig. 2).

In the Tri jezerca quarry only the upper part, about 10 m thick, of these limestones crops out (Fig. 15). In the uppermost part there are indications of a relative sea-level fall, and the beginning of a regression phase culminating in the regional Late Aptian emersion. Besides intense vertical bioturbation, indicating lowered sedimentation rates, weakly expressed palaeokarstification effects occur. A further relative sea-level fall resulted in a clearly visible emersion with palaeokarstified relics of *Istarski žuti*, greenish–grey clays in palaeokarst pits and/or coarse brecciated regolith. This unit represents a stratigraphic gap, which started during the Middle Aptian and lasted until the beginning of the Late Albian (VELIĆ & TIŠLJAR, 1987; VELIĆ et al., 1989).

Greenish–grey clays in the Tri jezerca quarry are up to 93 cm thick, and are situated in palaeokarst pits. Morphologically, pits are conical and compound, and resemble those recognized in the Late Dinantian palaeokarst of England and Wales, where VANSTONE (1988) recognized four types of palaeokarst depression morphology. We can tentatively conclude that the morphology of palaeokarst in the Tri jezerca quarry resembles that of hummocky palaeokarstic depressions. We consider that the clays are the erosional remains of surficial soils and sediments, which were accumulated in palaeokarst pits following an oscillating marine transgression that terminated emergence. Samples of greenish–grey clay (5BG 4/1 to 10BG 6/1 – MUNSELL COLOUR CHARTS, 1994) were taken along one profile for detailed analyses (Fig. 16). A sample of limestone (*Istarski žuti*) situated immediately bellow the clay was also collected.

Clays are composed of phyllosilicates and pyrite (Table 6). Gypsum was detected only in the uppermost sample. The clay mineral distribution along the profile shows a clear trend (Fig. 17). The main clay mineral in the upper part is illitic material (Fig. 18). In the lower part of the profile illite values are below 50 wt.%. The second main clay mineral group are regularly ordered and randomly ordered illite/smectite mixed-layer minerals. Chlorite is sub-

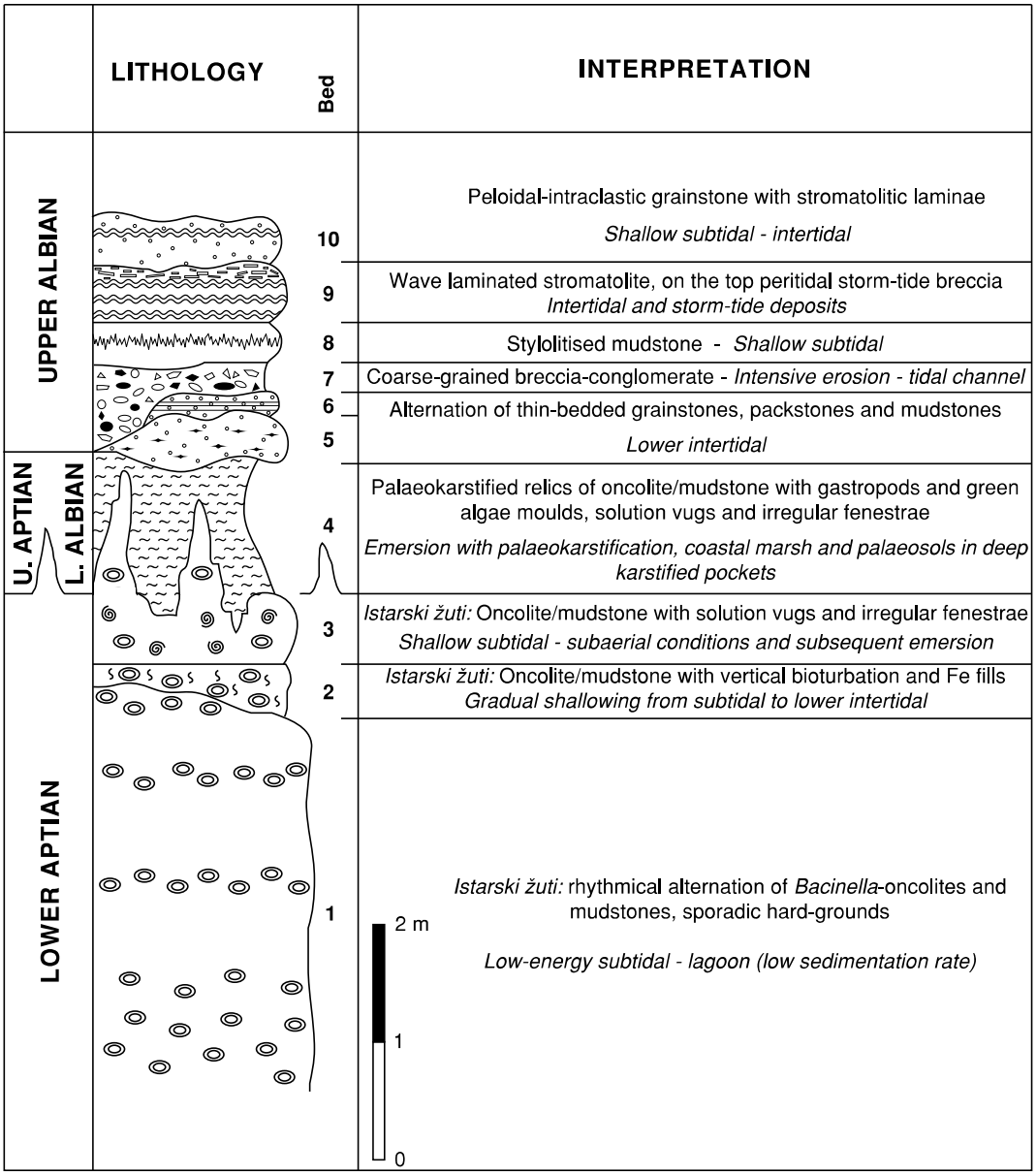

Fig. 15 Detailed geological column of the Lower Aptian *Istarski žuti* limestones, Late Aptian–Early Albian emersion with palaeokarstification and palaeosoil, and Upper Albian deposits in the Tri jezerca quarry (partly modified after TIŠLJAR et al., 1995).

		Phyllosilicates	Pyrite	Gypsum
1	0–8 cm	97	1	2
2	8–16 cm	97	3	
3	16–20 cm	98	2	
4	20–30 cm	99	1	
5	30–40 cm	99	1	
6	40–50 cm	99	1	
7	50–60 cm	99	1	
8	60–70 cm	99	1	
9	70–80 cm	99	1	
10	80–90 cm	99	1	
11	90–93 cm	99	1	
IRL		100		

Table 6 Semiquantitative mineral composition of greenish–grey clays from Tri jezerca quarry taken along a 93 cm thick profile. Sample 1 is uppermost and 11 is the lowermost sample. Legend: IRL) insoluble residue of limestone (Istarski žuti) situated immediately bellow clay.

ordinate and present only in the lower part of the profile. The insoluble limestone residue is dominated by smectite and illitic material (Table 6 and Fig. 17). In contrast to the clays, mixed-layer minerals were not detected in the insoluble limestone residue. The higher content of illitic material in the upper part of the profile corresponds well with chemical data. Namely, the K_2O-content in the upper part is around 5 wt.% and decreases to 4 wt.% in the lower part of the profile (Fig. 19).

Lower Cretaceous deposits of Istria, characterized by shallow-marine deposition, sporadically interrupted by periods of emersion, are sedimentologically and palaeogeographically very similar to some Jurassic–Cretaceous marine carbonate sequences of NW Europe, called Purbeckian sediments. Important members of these sediments are greenish–grey marls, which form thin films between limestone beds (DECONINCK et al., 1988). According to DECONINCK & STRASSER (1987) they are characterized by a mineralogical composition of smectite–illite–kaolinite, and usually occur at the top of small

Fig. 16 Greenish–grey clays in the Tri jezerca quarry. Cleaned profile prepared for detailed sampling.

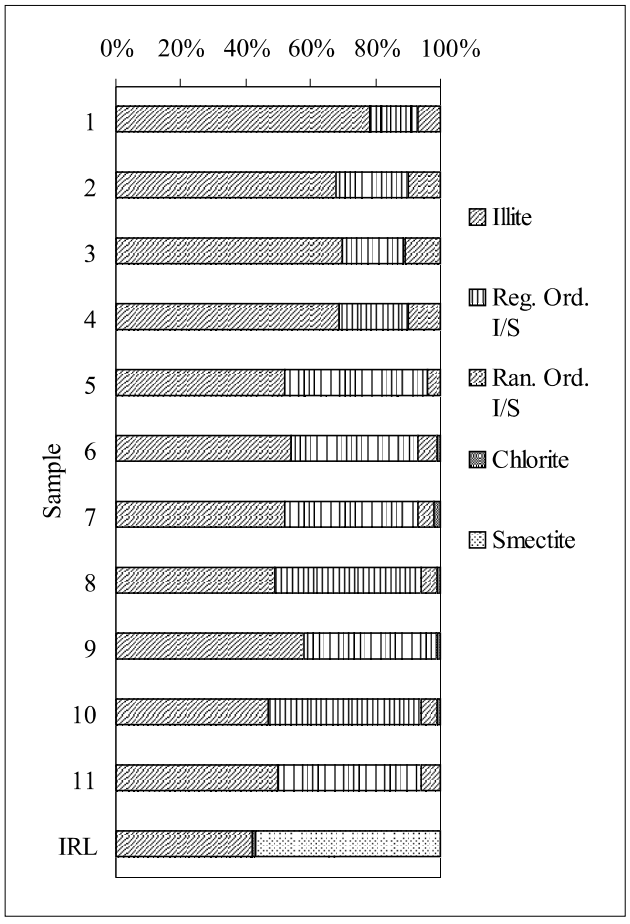

Fig. 17 Clay mineral composition of the <2 µm fraction along the profile in the Tri jezerca quarry.

shallowing-upward sequences. They may also have been subaerially exposed for a long period. DECONINCK et al. (1988) noted that even in sections showing illite-rich clay-assemblages underlying formations contain smectite and kaolinite. This led them to the conclusion that the influence of burial diagenesis on the illitization of smectite seems to be negligible in the Jura Mountains. Namely, although illitization of smectites is commonly attributed to increasing temperature as burial diagenesis proceeds (HOWER et al., 1976), EBERL et al. (1986) suggested that K-fixation necessary for illitization of smectites could be achieved at surface temperatures by repeated wetting and drying. This led ROBINSON & WRIGHT (1987) to suggest that some mixed-layer illite/smectite could be produced from smectite during pedogenesis. DECONINCK et al. (1988) noted that illite occurred in areas closer to marine influences, and suggested that illite was formed by conversion from detrital smectite, as a result of repeated wetting by K-rich marine waters and subsequent drying in a hypersaline environment. The K^+ necessary for illitization of smectite was probably provided by marine waters, plant debris washed into ponds, leaching of volcanic rocks and from various other sources (DECONINCK et al., 1988).

The clay mineral composition of clays in the Tri Jezerca quarry clearly indicates the influence of both pedogenic and diagenetic processes. Mineralogical as well as chemical data indicate that transformation of smectite (from the mixed-layer minerals) to illite must have occurred. Wetting and drying experiments and layer charge measurements support this theory (Figs. 20 and 21). K-fixation necessary for illitization of smectites could have been achieved on the palaeolandscape by repeated wetting and drying. Potassium may have been provided by plants, marine waters, volcanic dust and other sources.

Based on micromorphological research, it can also be concluded that greenish–grey clays from the Tri jezerca quarry were pedogenetically altered, i.e. they are palaeosols. The following facts favour this statement: (i) weakly developed soil structure (Fig. 22), (ii) presence of root remains, burrows and channels, now mainly filled with pyrite framboids (Fig. 23), (iii) nests of the faecal products of soil dwelling fauna, (iv) nodular pedofeatures (Fig. 24), and (v) microfabric (Figs. 25 and 26). The colour of palaeosols, the presence of root remains only in the upper part of the profile and high abundance of pyrite framboids may imply that they were probably seasonally marshy soils (partly or

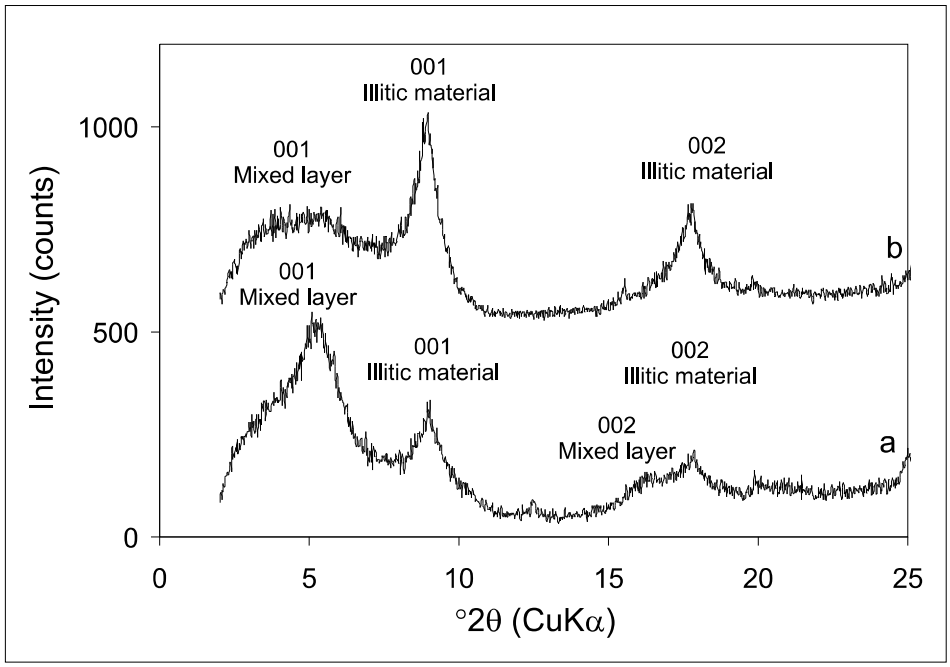

Fig. 18 Characteristic parts of XRD patterns of selected clay samples (<2 μm fraction) from Tri jezerca quarry: (a) upper part of profile, sample 1, glycol solvated; (b) lower part of the profile, sample 10, glycol solvated.

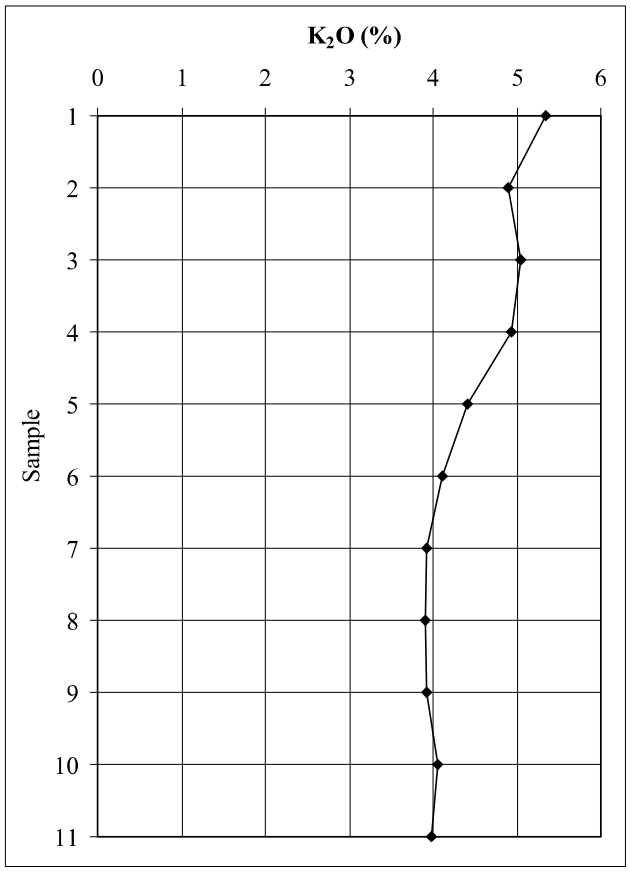

Fig. 19 Distribution of K_2O (in wt.%) along the profile in the Tri jezerca quarry.

wholly within the zone of water-table fluctuation), to permanently waterlogged soil (entirely below the water-table). This is also supported by the distribution of U, V and Mo along the profile (Fig. 27) and REE distribution. The total REE content of the clay profile ranges from 87.80–123.56 ppm. $(La/Yb)_{ch}$ ratios in grey waterlogged palaeosols vary from 4.51–6.82 and are significantly lower than that of ES indicating HREE enrichment relative to LREE (Fig. 28). The total REE content in the insoluble residue of limestone is 148.04 ppm and the $(La/Yb)_{ch}$ ratio is 15.67. Enrichment of HREE in clays from the Tri jezerca quarry is probably the result of the higher mobility of LREE in an acidic pedogenic environment. Very low values of $\delta^{34}S$ in pyrites ($\delta^{34}S$ is -36‰) from the Tri jezerca quarry (sample SB2; 8–16 cm, Fig. 23) may also result from repeated cycles of oxidation and reduction, i.e. fluctuation of the water-table in wetland marshy soils.

The parentage of the material from which this soil was formed is still uncertain, but there are clear indications that materials other than the insoluble residue of limestones (e.g. volcanic dust, Fig. 29) may have contributed to the genesis of these clays. For example the Zr/Nb ratios in the insoluble limestone residue are much lower than these ratios in clays from the Tri jezerca quarry (Fig. 30). Namely, if we consider Zr and Nb as relatively immobile in soil (MUHS et al., 1987, 1990), then parent materials other than the insoluble residue of limestones may have influenced clay composition. This is also supported by the clay mineralogy results (Fig. 17).

The beginning of Upper Albian deposition (Fig. 15) is characterized by an oscillating transgression, and alternations of peritidal fenestral mudstones, fossiliferous wackestones and packstones, and high-energy shoreline and tidal-channel fill conglomerates and black-pebble breccias (TIŠLJAR et al., 1995). Within these sediments, features indicating 2 short emersions, represented mainly by coarse brecciated zones infilled with greenish–grey and greenish–yellow clays can be observed. The clay mineralogy of these clay infillings is similar to that of the lowest part of the greenish–grey clay situated in a palaeokarst pit (Fig. 17). E.g., the main clay minerals in clay infillings from the first brecciated zone are regularly ordered and randomly ordered illite/smectite mixed-layer minerals (52 wt.%). They are followed by illitic material (48 wt.%). These clays do not contain pyrite and chlorite.

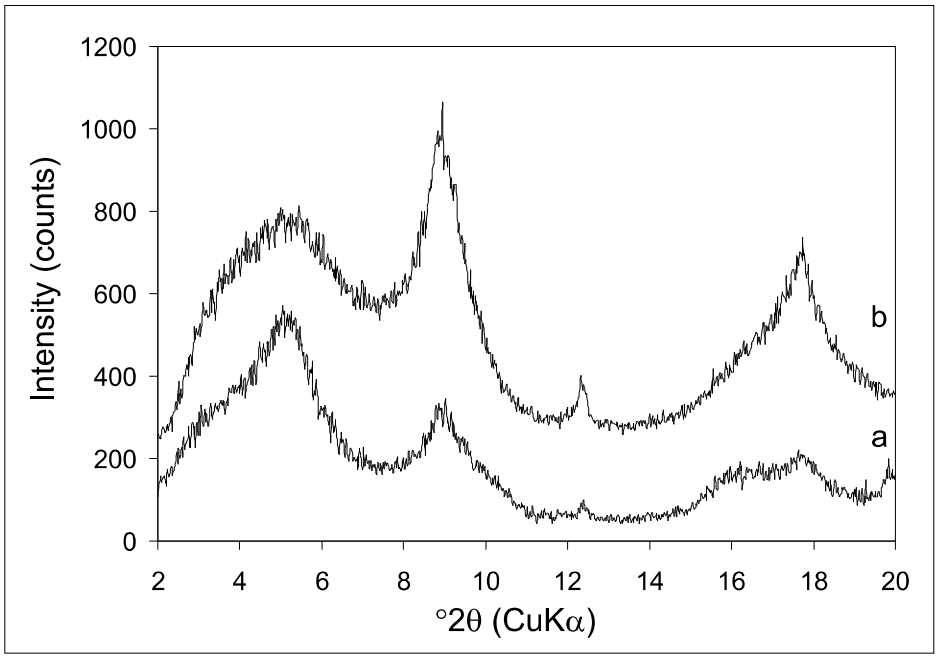

Fig. 20 Characteristic parts of XRD patterns of clay sample 10 (<2 μm fraction) from Tri jezerca quarry: (a) Sr treated, glycol solvated, after 0 wetting/drying cycles; (b) Sr treated, glycol solvated, after 100 wetting/drying cycles.

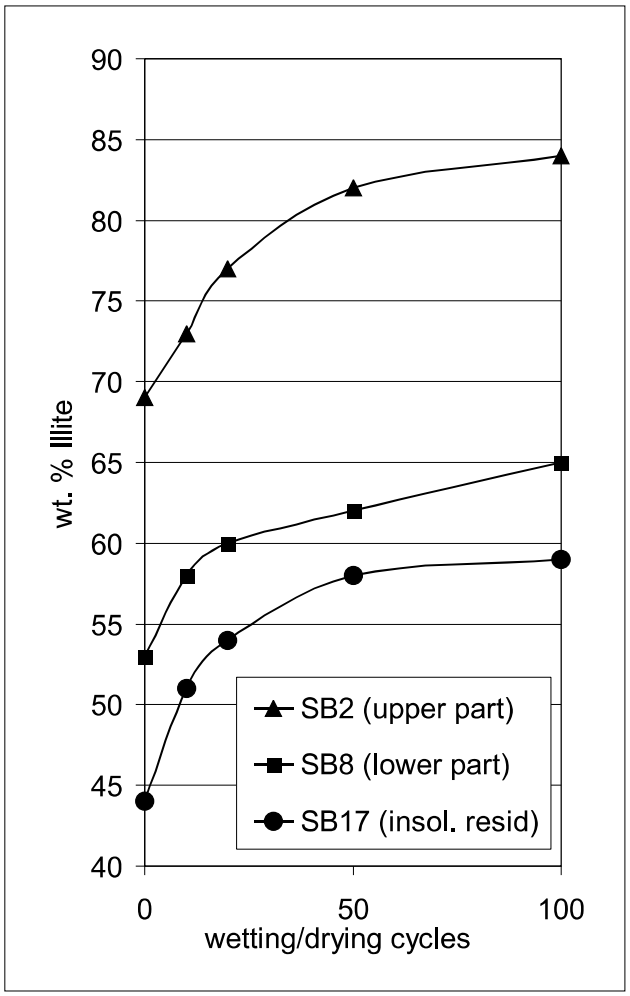

Fig. 21 The content of illitic material in selected clay samples from Tri jezerca quarry and in underlying limestone (insoluble residue) after 0 to 100 wetting/drying cycles.

Fig. 22 Contact between greenish–grey clays and karstified "Istarski žuti" limestone (Tri jezerca quarry).

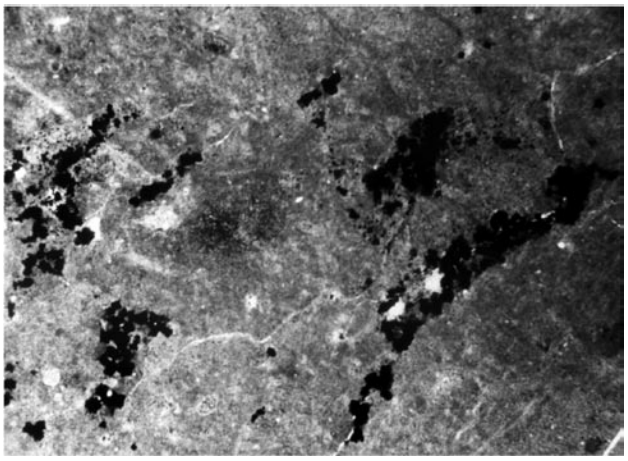

Fig. 23 Root remains, burrows and channels, mainly filled with pyrite framboids (upper part of profile shown on Fig. 25, 10–18 cm, Tri jezerca quarry); length of photograph = 3.3 mm.

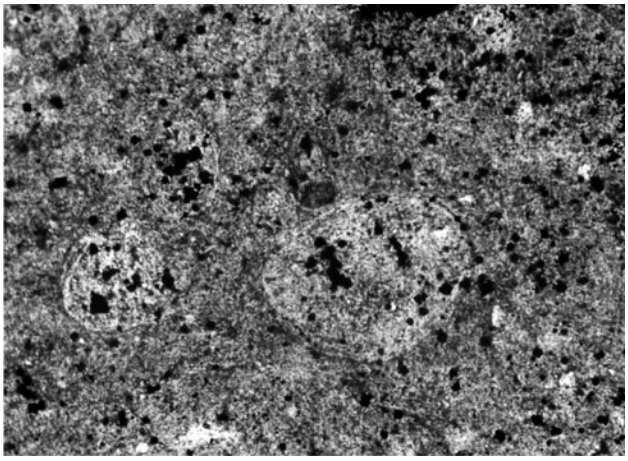

Fig. 24 Nodular pedofeatures (upper part of profile shown on Fig. 25, 10–18 cm, Tri jezerca quarry); length of photograph = 3.3 mm.

Fig. 25 Bright clay strikes may correspond to cross-striated b-fabric and masepic plasmic fabric (upper part of profile shown on Fig. 25, 0–8 cm, Tri jezerca quarry); crossed nicols, length of photograph = 3.3 mm.

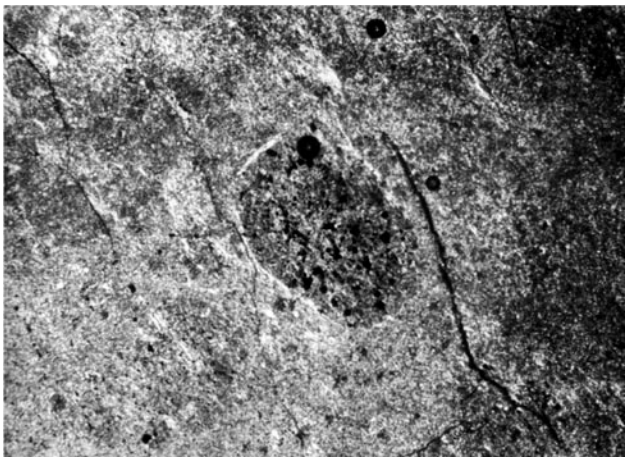

Fig. 26 Some of the features in the clayey matrix show the outline of former crystals, now replaced by clay (upper part of profile shown on Fig. 25, 10–18 cm, Tri jezerca quarry); crossed nicols, length of photograph = 3.3 mm.

4. QUATERNARY SEDIMENTS AND SOILS ON THE JURASSIC–CRETACEOUS–PALAEOGENE CARBONATE PLAIN OF SOUTHERN AND WESTERN ISTRIA

4.1. Introduction

Since the end of the Eocene (or probably earlier for the central parts of Istria – MATIČEC et al., 1996) the surface of the Istrian Peninsula has been affected by karst processes and weathering, which has led to the development of both surficial and underground features. Different types of sediments, polygenetic palaeosols and soils have been formed. Among them the most important are loess and *terra rossa*. The oldest Quaternary sediments were discovered in the Šandalja cave near Pula, and are represented by red breccia with faunal remains of Early Pleistocene age (MALEZ, 1981). According to CREMASCHI (1990a) deposition of loess was a very important recurrent process in Northern and Central Italy from at least the early Middle Pleistocene. He recognized the following loess depositional periods: (1) Middle Pleistocene; (2) Upper Pleistocene, with two main phases of loess sedimentation: the first during Early Pleniglacial and second during the Second Pleniglacial, and (3) Younger Dryas (Late-glacial loess). Loess deposition also affected Istria. Loess is situated in the southern (Premantura and Mrlera) and northwestern parts of Istria (Savudrija) and is considered to be Upper Pleistocene in age (POLŠAK, 1970). Although there are no data about older loess deposits in Istria, they were recognized on the neighbouring Island of Susak. They are situated below the Upper Pleistocene loess and have a reddish alfisol developed on their top, which is thought to have formed in the Riss–Würm interglacial (CREMASCHI, 1990b).

Terra rossa is a common general term used among Croatian geologists and pedologists for reddish soil occurring on limestone and dolomite substrates. The nature and relationship of *terra rossa* to underlying carbonates is a long-standing problem, which has resulted in different opinions with respect to the parent material and origin of *terra rossa*. The bright red colour is a diagnostic feature of *terra rossa* and is a result of the preferential formation of haematite over goethite, i.e. *rubification*. Generally, *terra rossa* can be, according to different authors, considered as soil, relict soil (non-buried-palaeosol), palaeosol or a

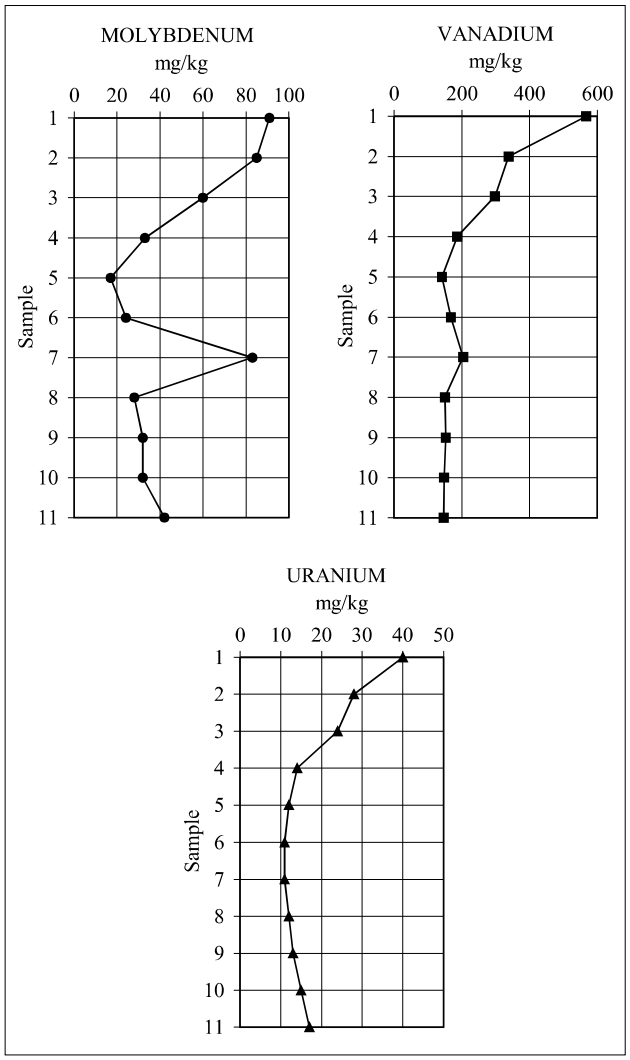

Fig. 27 Distribution of Mo, U and V along along the profile in the Tri jezerca quarry.

pedo–sedimentary complex (soil-sediment). Most authors today believe that *terra rossa* is a polygenetic relict soil formed during the Tertiary and/or hot and humid periods of the Quaternary. However, some recent investigations (e.g. BRONGER & SEDOV, 2002) show that at least some *terra rossa* previously referred to as polygenetic relict soils should be regarded as Vetusols (soils which are marked by a continuity of pedogenetic processes in time), in accordance with the concept of CREMASCHI (1987). According to DURN et al. (1999), in some isolated karst terrains *terra rossa* may have formed exclusively from the insoluble residue of limestone and dolomite, but much more often it comprises a span of parent materials which derived from carbonate terrains via different transport mechanisms.

Terra rossa is found on the Jurassic–Cretaceous–Palaeogene carbonate plain of southern and western Istria. It fills cracks and sinkholes, and forms a discontinuous surface layer up to 2.5 metres thick. Since *terra rossa* has been exposed to various climatic fluctuations it can be affected by aeolian deposition, erosion, colluviation, eluviation, yellowing and secondary hydromorphy. Erosion and depositional processes which were superimposed on karst terrains and induced by climatic changes, tectonic movements and/or deforestation might be responsible for both the patchy distribution of *terra rossa*, and thick colluvial accumulations (up to 14 m) of *terra rossa*-like materials, in *uvala* and *dolina* types of karst depressions (pedo–sedimentary complexes, soil-sediments).

The Upper Pleistocene loess in the northwestern part of Istria (Savudrija cape) covers red interglacial palaeosols and *terra rossa*. This indicates that the Upper Pleistocene loess post-dated *terra rossa* formation in Istria. However, the presence of aeolian dust was also recognized in the upper part of *terra rossa* in areas where loess is not present, or not clearly recognized (DURN, 1996). Namely, when the rate of aeolian dust accumulation increases to 40 μm/y, dust accumulates as surface loess (YAALON, 1997). When the rate of accumulation is less than 20 μm/y the accreted dust manages to become completely assimilated by the prevailing pedoenvironment, and is leached or bioturbated into the soil profile (YAALON, 1997). This is why the addition of aeolian dust to a soil is usually difficult to identify. If we bear this in mind, it can be postulated that similar external materials might have contributed to *terra rossa* since the Middle Pleistocene. Consequently, DURN et al. (1999) presented evidence for the polygenetic nature of *terra rossa* in Istria, based on detailed mineralogical and geochemical investigation. Namely, neither the content and particle size distribution nor the bulk and clay mineralogy of the insoluble residue of limestone and dolomite support development of *terra rossa* entirely by dissolution of carbonate rocks. They concluded that both aeolian sediments older than those of Upper Pleistocene age and flysch might have contributed to the genesis of *terra rossa*. DURN et al. (1999) also found that arithmetic means of two populations (Fe_d of 45 *terra rossa* samples from various locations around the world and Fe_d of 40 samples from Istria) represent two independent estimates of the same population (Fe_d in *terra rossa*), and concluded that this supports BOERO & SCHWERTMANN's (1989) conclusion that the rather limited extent of variation of selected Fe-oxide characteristics may indicate a specific pedoenvironment in which *terra rossa* is formed. They suggested that this pedoenvironment is characterized by an association of Mediterranean climate, high internal drainage due to the karstic nature of a hard limestone, and neutral pH conditions.

In the frame of this excursion we will see polygenetic relict *terra rossa* soil in Novigrad (Stop 3).

4.2. Stop 3: Polygenetic relict *terra rossa* soil in the Novigrad town area (western Istria)

The Novigrad profile is situated on the coast of Novigrad bay, NW of Novigrad town (Fig. 4). It represents a polygenetic *terra rossa* soil about 150 cm thick, situated on fine-grained pelletal wackestone of Lower Cretaceous age (Upper Albian, Fig. 31). In the lowest part of the profile it is clear that the limestones were exposed to the process of rubification (Fig. 32). Dissolution voids and cracks in limestone at the contact with *terra rossa* are infilled exclusively with clayey matrix (Fig. 33). A detailed description of the Novigrad profile is presented in Fig. 34. The chemical composition and selected weathering indices of samples from Novigrad are given in Tables 7 and 8 and Fig. 35.

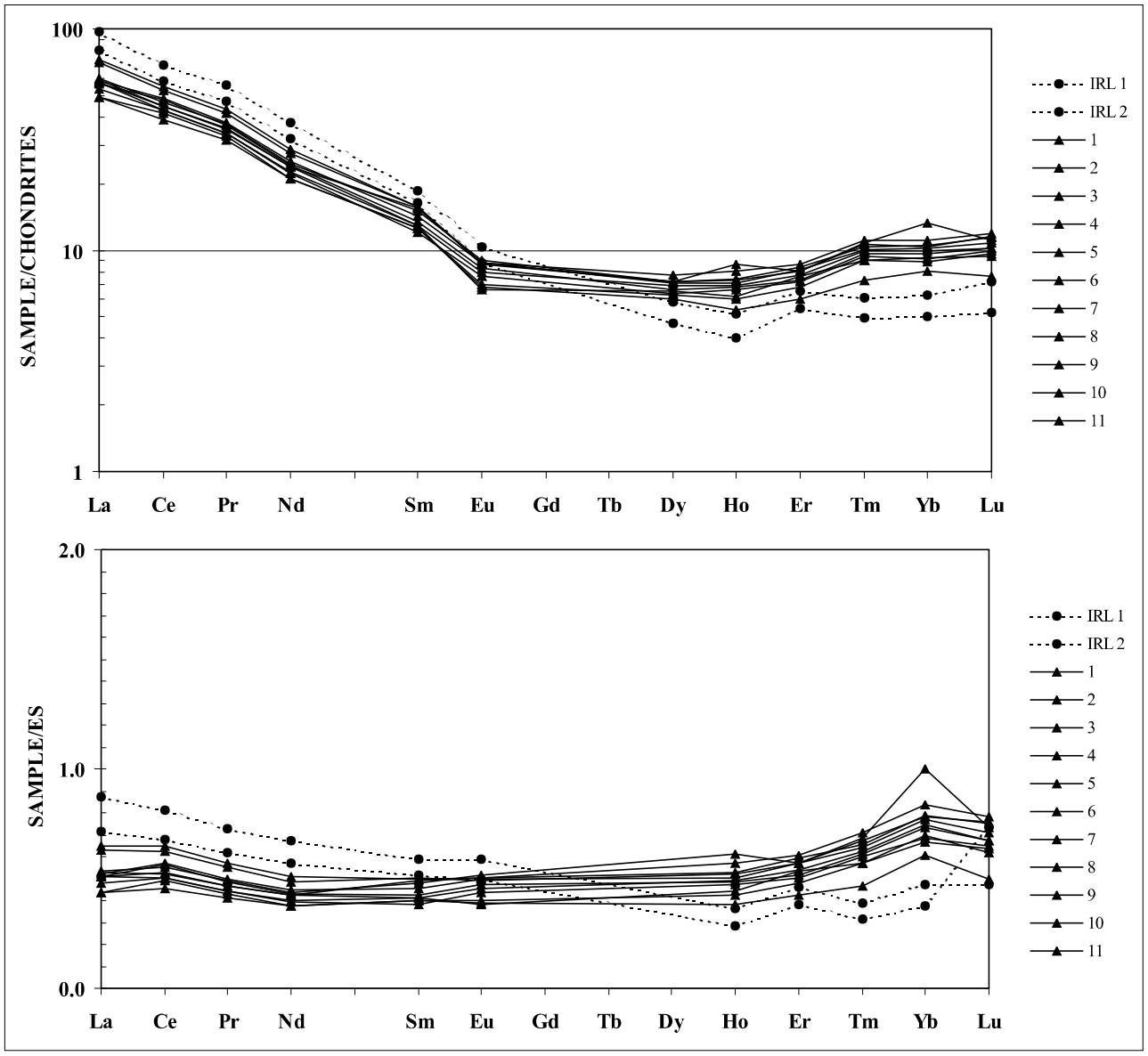

Fig. 28 Chondrite-normalized and European shale-normalized REE patterns of greenish–grey clays from the Tri jezerca quarry and the insoluble residue of limestone from the Tri jezerca and Kanfanar quarries (numbers of samples match those on Figs. 27 and 28). Legend: IRL1) insoluble residue of limestone (Istarski žuti) situated immediately bellow clay in the Tri jezerca quarry (Stop 2); IRL2) insoluble residue of limestone (Istarski žuti) situated immediately bellow clay in the Kanfanar quarry.

The contents of SiO_2, TiO_2, MnO and Na_2O are significantly higher, and Al_2O_3 and Fe_2O_3 lower in the upper part of the profile (Fig. 34 and Table 7; samples 131 and 132, horizons IIB1 and IIB2). A clear trend of decreasing content of SiO_2 and Na_2O and increasing content of Al_2O_3 and Fe_2O_3 both in the upper and lower part of profile (samples 133, 134, 135 and 136; horizons IIIB1t, IIIB2t, IIIB3t and IIIB4t(g)) is observed. Distribution of MgO and P_2O_5 do not show a clear trend with depth.

Weathering indices also show clear trends in the distribution of the major elements (Table 8). Although K_2O does not show a clear trend along the profile, decreasing content of Na_2O with depth is also manifested as a decrease in the Na_2O/K_2O index with depth. The same trend is observed for other weathering indices. The trends of increasing contents of Al_2O_3 and Fe_2O_3, and decreasing contents of SiO_2 and Na_2O with depth are compatibile with the increasing amount of the clay fraction with depth (Table 8).

Both the upper and lower parts of the profile are mineralogically similar. They consist of quartz, plagioclase, K-feldspar, micaceous clay minerals (illitic material and mica), kaolinites (Kl_D and Kl), vermiculite, mixed-layer clay minerals (other than illitic material), haematite, goethite and an XRD-amorphous inorganic compound (Tables 9 and 10). However, the content of quartz and plagioclase is higher in the upper part, while the content of phyllosilicates and Fe-oxides is higher in the lower part of the profile. Dominant mineral phases in the clay fraction of the Novigrad profile are kaolinites (Kl_D and Kl) and illitic material, while vermiculite, mixed-layer clay minerals and quartz are present in subordinate amounts (Figs. 36 and 37). The content of kaolinite which does not form intercalation compounds with DMSO (Kl) is higher than that of kaolinite which intercalates with DMSO (Kl_D) (Fig. 37). The K_2Ox100/Al_2O_3 index, which can be in this case considered as a good approximation of the illite/kaolinite

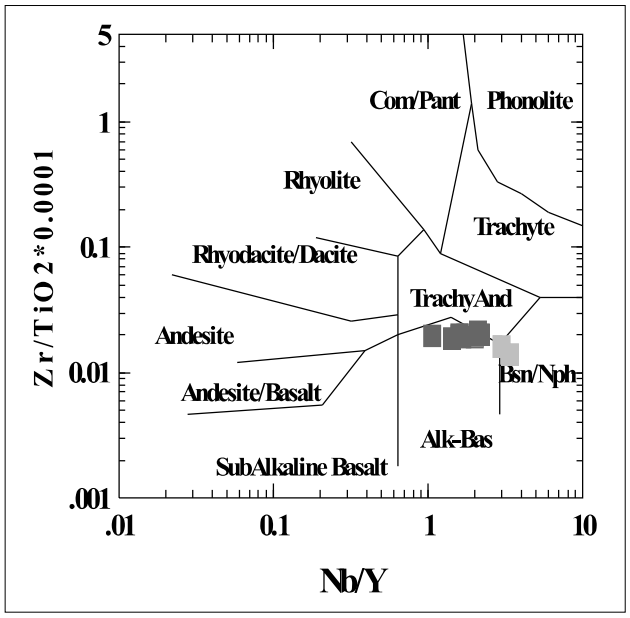

Fig. 29 Diagram after WINCHESTER & FLOYD (1977) for greenish–grey clays from Tri jezerca quarry (dark grey) and insoluble residue of limestone from the Tri jezerca quarry and Kanfanar quarry (light grey.

ratio (MORESSI & MONGELLI, 1988), decreases downvards (Table 8). This indicates that the amount of kaolinite increases downwards. DURN et al. (1999) concluded that kaolinite which does not form intercalation compounds with DMSO(Kl) is the dominant mineral phase in the fine clay of *terra rossa* in Istria and is considered predominantly authigenic rather than being inherited from parent materials.

Samples from the Novigrad profile bear typical *terra rossa* Fe-oxide characteristics, e.g. Fe_d and Fe_d/Fe_t (DURN et al., 1999). Fe_d/clay ratios are relatively uniform along the profile and clearly indicate a predominance of co-illuviation of clay and Fe oxides, i.e. connection of Fe-oxides with the clay fraction (DURN et al., 2001). So, translocation of clay particles is responsible for the distribution of the red colour through the whole profile.

In order to characterize chemically insoluble residues of carbonate rocks and compare them with *terra rossa* and loess, DURN et al. (1999) among others also used Zr and Nb, elements with a high ionic potential which are considered relatively immobile in soil environments and suitable for geochemical "fingerprinting" (MUHS et al., 1987, 1990). Zr/Nb ratios in the insoluble residue of Jurassic and Cretaceous limestones and dolomites are generaly lower than these ratios in the Novigrad profile, although there is obvious overlapping of the lower part of the Novigrad profile with the insoluble residue field (Fig. 30).

The heavy mineral fraction of the Novigrad profile is enriched in epidote–zoisite group minerals, amphiboles and garnets (Fig. 38, samples 131, 134 and 136), which may indicate that at least part of the parent material from which *terra rossa* was formed belongs to the Po plain–Adriatic loess region provenance. However, the contents of epidote–zoisite group minerals, amphibole and garnet decreases, while contents of zircon, tourmaline and rutile increases with depth along the profile. This may indicate that the parent material is of mixed provenance. The content of the clay fraction in the highly weathered loess from Northern and Central Italy ranges from 58–75 wt.% and that of the sand fraction from 1–3 wt.% (CREMASCHI, 1990b). These results are very similar to the results obtained for *terra rossa* (Fig. 39). DURN et al. (2003) tentatively attributed red interglacial soil situated below the Savudrija loess complex, (which has significantly higher silt/clay ratios than *terra rossa* in the Novigrad profile, Table 8) to the Eemian interglacial period. There is sufficient evidence to propose that formation of *terra rossa* started earlier than this.

Materials other than the insoluble residue of limestones and dolomites which have contributed to *terra rossa* in Istria are aeolian sediments, the deposition of which was a very important recurrent process in Istria probably since the early Middle Pleistocene, and flysch sediments which extended further south from its present position (DURN et al., 1999). Based on detailed heavy mineral study, DURN et al. (2006) concluded that the main external contributor to *terra rossa* in Istria is Middle Pleistocene loess, followed by flysch and tephra (minor contributions). Upper Pleistocene loess might have become intermixed in the upper parts of already formed *terra rossa*.

Terra rossa is formed as a result of: (1) *decalcification*, (2) *rubification* and (3) *monosiallitization* (neoformation of kaolinite). However, since they have been exposed to vari-

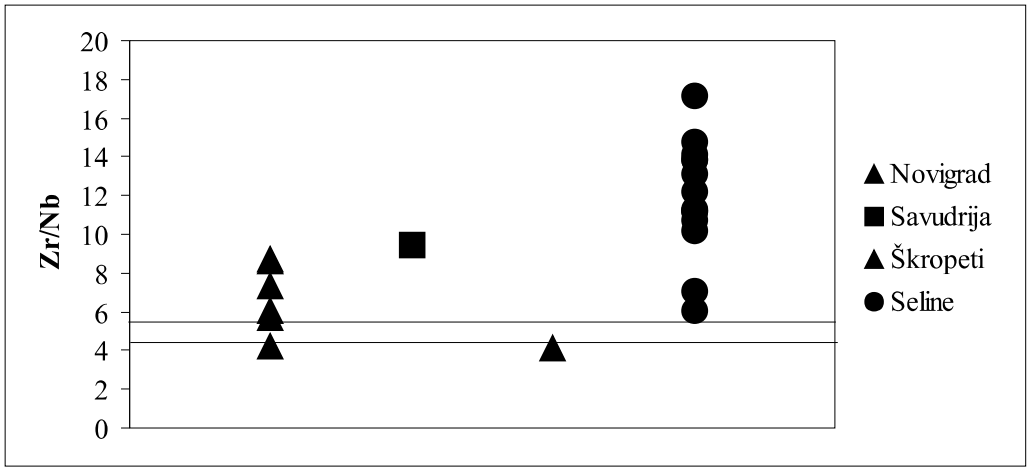

Fig. 30 Zr/Nb ratios for greenish–grey clays from the Tri jezerca quarry (Seline) and *terra rossa* (Novigrad, Savudrija and Škropeti). Two horizontal lines represent the minimum and maximum values for these ratios in insoluble residues of limestone. Data for *terra rossa* and insoluble residues of limestone from DURN et al. (1999).

Fig. 31 Polygenetic *terra rossa* soil in Novigrad. Cleaned profile prepared for detailed sampling.

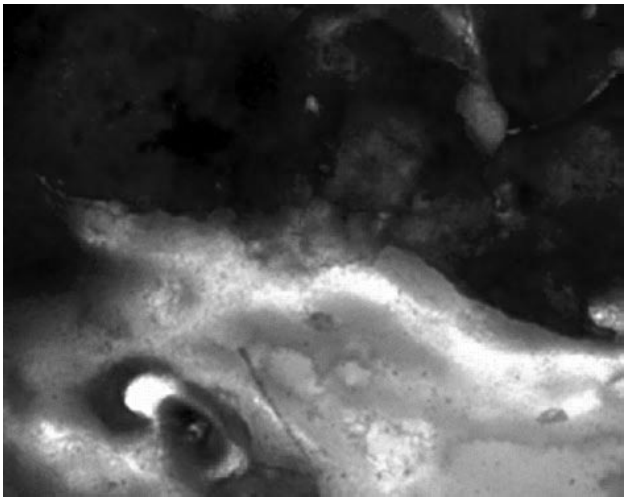

Fig. 32 *Terra rossa* and footwall limestone contact. Novigrad profile. Depth=150 cm. Length of photograph=1.5 mm.

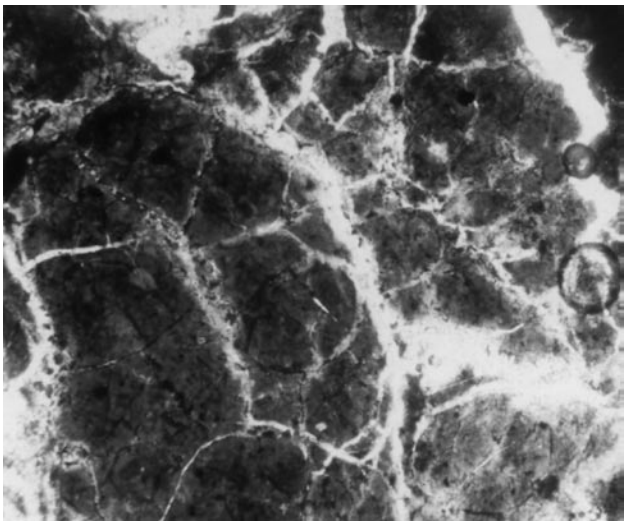

Fig. 33 Fissure microstructure. Basic mass consists of micromass only. Novigrad profile. Depth=145 cm. Length of photograph=7.5 mm.

ous climatic fluctuations *terra rossa* soils can be affected by aeolian deposition, erosion, colluviation, eluviation, yellowing and secondary hydromorphy (gleyzation). For example, pedorelics found in *terra rossa* may be the erosional remains of very old (from Miocene on?) soils formed exclusively from the insoluble residue of limestones and dolomites. Now they represent only one component of a fine colluvium, which may also contain erosional remains of other pre-existing soils, aeolian sediments (of different ages), flysch and bauxites.

Based on the field description of the profile and the laboratory analyses, we may conclude that the Novigrad profile represents a typical polygenetic *terra rossa* soil.

5. REFERENCES

BÁRDOSSY, Gy. (1982): Karst Bauxites, Bauxite Deposits on Carbonate Rocks.– Developments in Economic Geology, 14, Elsevier, Amsterdam, 441 p.

BÁRDOSSY, Gy. & DERCOURT, J. (1990): Les gisements de bauxite tethysiens (Mediterranée, Proche et Moyen Orient); cadre paleogeographique et controles genetiques.– Bull. Soc. Geol. France (8), 4/6, 869–888.

sample	SiO_2	TiO_2	Al_2O_3	Fe_2O_3	MnO	MgO	CaO	Na_2O	K_2O	P_2O_5	LOI	SUM
131	59.46	1.29	17.57	5.78	0.19	0.81	0.74	0.40	1.61	0.15	12.42	100.6
132	58.82	1.26	18.59	5.89	0.18	0.80	0.69	0.38	1.58	0.13	11.29	99.66
133	50.27	1.06	22.76	8.68	0.10	0.86	0.73	0.26	1.65	0.12	13.35	99.89
134	50.27	1.08	22.67	8.75	0.10	0.88	0.67	0.26	1.65	0.13	13.56	100.1
135	49.84	1.08	23.06	8.87	0.08	0.86	0.66	0.23	1.63	0.13	13.41	99.90
136	47.91	1.01	23.39	9.31	0.10	0.85	0.64	0.18	1.55	0.12	14.82	99.93

Table 7 Chemical composition (major elements) of samples from polygenetic *terra rossa* soil (Novigrad profile). For sample description see Fig. 34. Data from DURN (1996).

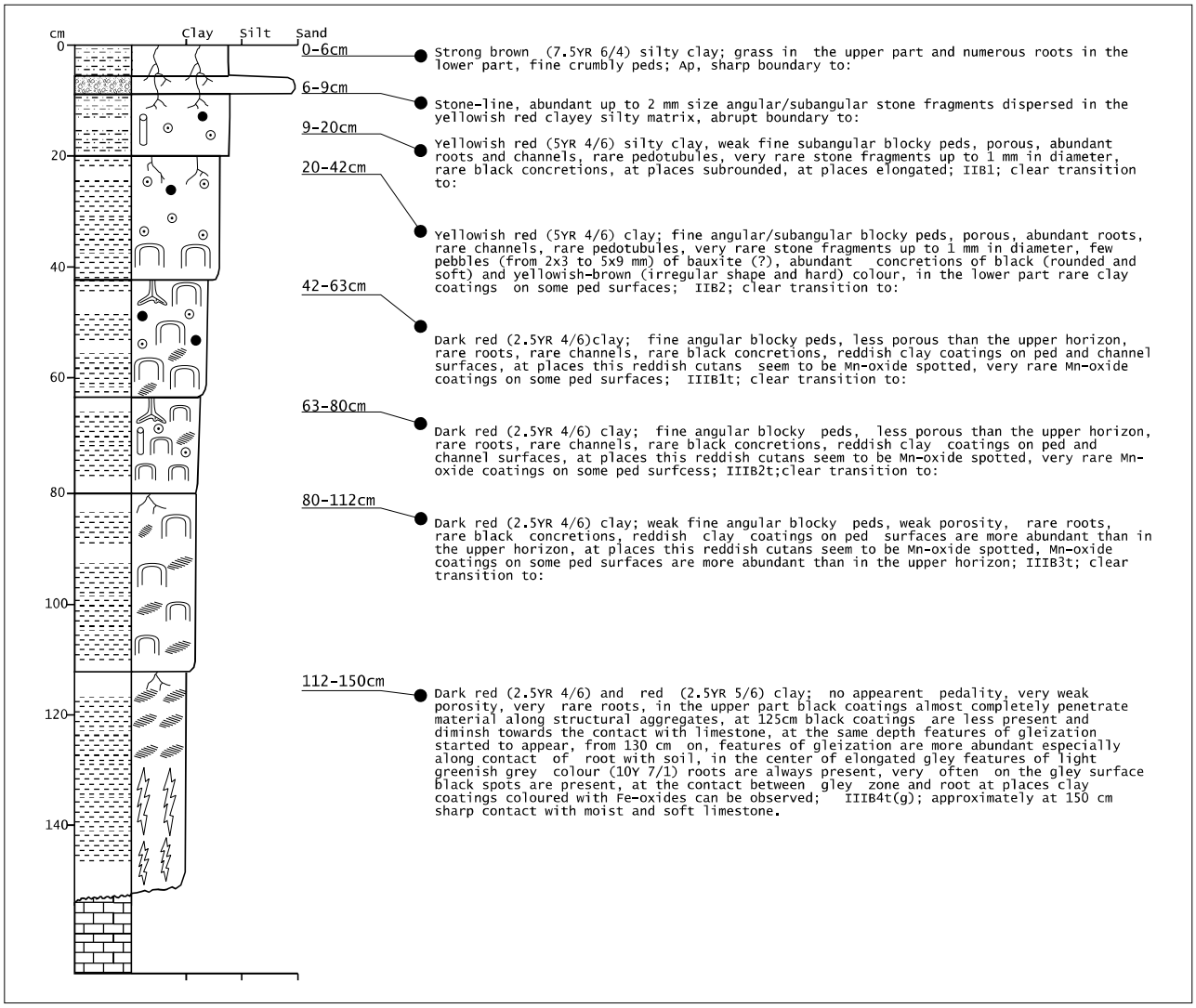

Fig. 34 Field description of polygenetic *terra rossa* soil (Novigrad profile). Modified from DURN (1996).

BERNOULLI, D. (2001): Mesozoic–Tertiary carbonate paltforms, slopes and basins of the external Appennines and Sicily.– In: VAI, G.B. & MARTINI, I.P. (eds.): Anatomy of an Orogen: the Appennines and Adjacent Mediterranean Basins. Kluwer Academic Publ., 307–326.

BOERO, V. & SCHWERTMANN, U. (1989): Iron oxide mineralogy of terra rossa and its genetic Implications.– Geoderma, 44, 319–327.

BORDEA, S. & MANTEA, G. (1991): Stratigraphical composition of the bauxite deposits in the Padurea Craiului Mountains (northern Apuseni Mountains).– In: Tethyan Bauxites IGCP–287, part II., Acta Geol. Hung., 34/4, 351–376.

BRONGER, A. & SEDOV, S.N. (2002): Vetusols and paleosols: natural versus man-induced environmental change in the Atlantic coastal region of Morocco.– 17th World Conference on Soil Science, Paper no.1530, 1–12.

CARANNANTE, G., D'ARGENIO, B., MINDSZENTY, A., RUBERTI, D. & SIMONE, L. (1994): Cretaceous–Miocene shallow water carbonate sequences. Regional unconformities and facies patterns.– In: CARANNANTE, G. & TONIELLI, R.

sample	Na_2O/K_2O	$(CaO+MgO+K_2O+Na_2O)/Al_2O_3$	K_2Ox100/Al_2O_3	SiO_2/Fe_2O_3	silt/clay
131	0.38	0.33	9.16	27.34	0.77
132	0.37	0.30	8.5	26.54	0.64
133	0.24	0.25	7.25	15.39	0.41
134	0.24	0.25	7.28	15.27	0.36
135	0.21	0.24	7.07	14.93	0.35
136	0.18	0.23	6.63	13.68	0.28

Table 8 Weathering indices for samples from polygenetic *terra rossa* soil (Novigrad profile). For sample description see Fig. 34. Data from DURN (1996).

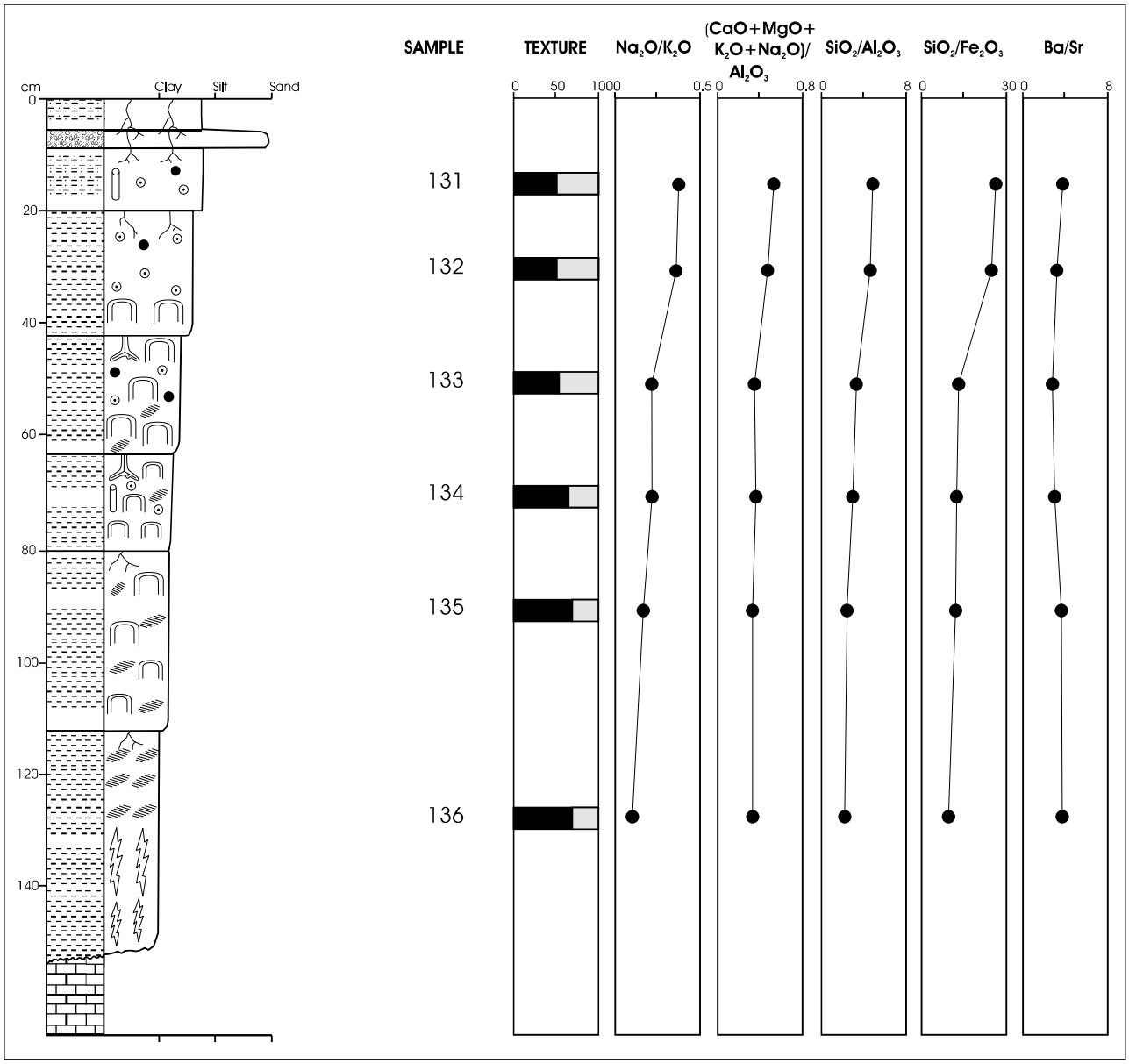

Fig. 35 Weathering indices for samples from polygenetic *terra rossa* soil (Novigrad profile). In column for texture black = clay content; grey = silt content. For sample description see Fig. 34. Modified from DURN (1996).

sample	Quartz	Plagioclase	K-feldspar	Haematite+Goethite	Phyllos.+am.
131	25	3	1	5	66
136	15	1	1	7	76

Table 9 Mineral composition of the <2 mm fraction of polygenetic *terra rossa* soil (Novigrad profile) in wt.%. Legend: Phyllos.+am.) phyllosilicates and amorphous inorganic compound. For sample description see Fig. 34. Data from DURN et al. (1999).

Sample	Illitic material	KI_D	KI	Vermiculite	Mc	Quartz
131	+	+	+	+	+	+
136	+	+	+	+	+	+

Table 10 Mineral composition of the <2 μm fraction of polygenetic *terra rossa* soil (Novigrad profile) after the removal of carbonates, humic materials and iron-oxides. Legend: KI_D) kaolinite which forms intercalation compounds with DMSO; KI) kaolinite which does not intercalate with DMSO; Mc) mixed-layer clay mineral. Data from DURN et al. (1999).

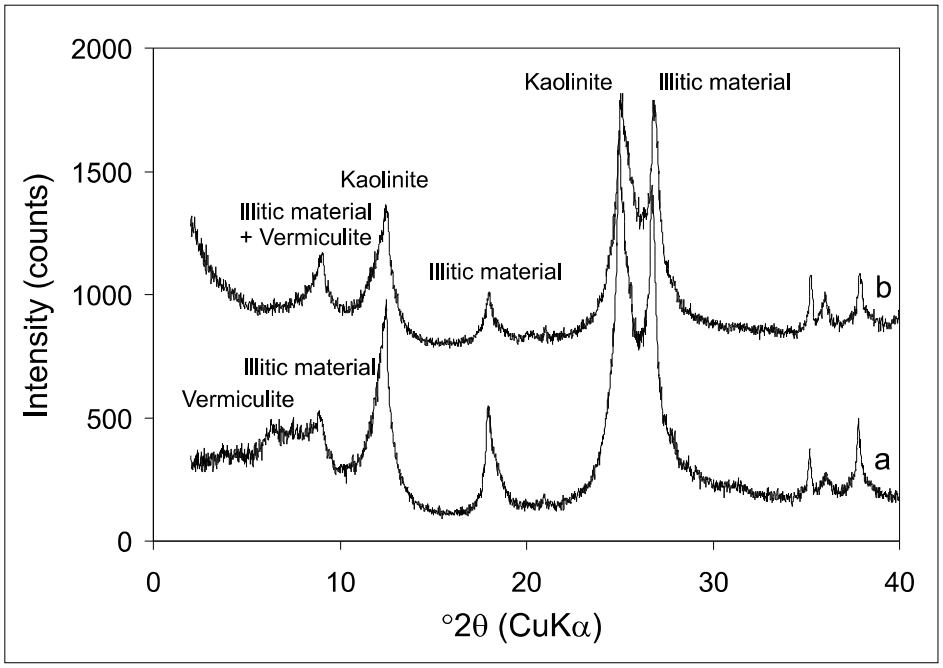

Fig. 36 Characteristic parts of XRD patterns of *terra rossa* sample 136 (<2 µm fraction): (a) Mg-saturated; (b) K-saturated.

(eds.): 15th IAS Regional Meeting, Ischia, Italy, Pre-Meeting Fieldtrip Guidebook, Exc. A2, 25–59.

CHANNEL, J.E.T. (1996): Paleomagnetism and paleogeography of Adria.– Geol. Soc. London, Spec. publ., 105, 119–132.

COMBES, P.J. (1990): Typologie, cadre geodynamique et genese des bauxites Francaises.– Geodinamica Acta (Paris), 4/2, 91–109.

COMBES J.-P. & BÁRDOSSY, Gy. (1994): Typologie et controle geodynamique des bauxites tethysiennes.– Compt. Rend. Acad. Sci. Paris, ser. II, 318, 359–366.

CREMASCHI, M. (1987): Paleosols and Vetusols in the central Po plain, a study in Quaternary geology and soil development.– Edizioni Unicopli, Milano, 306 p.

CREMASCHI, M. (1990a): Stratigraphy and palaeoenvironmental significance of the loess deposits on Susak island (Dalmatian Archipelago).– Quaternary International, 5, 97–106.

CREMASCHI, M. (1990b): The loess in northern and central Italy: a loess basin between the Alps and the Mediterranean regions.– In: CREMASCHI, M. (ed.): The Loess in Northern and Central Italy. Centro di Studio per la Stratigrafia e Petrografia delle Alpi Centrali, Editrice Gutenberg, Milano, 15–19.

D'ARGENIO, B. & MINDSZNETY, A. (1991): Karst bauxites at regional unconformities and geotectonic correlation in the Cretaceous of the Mediterranean.– Boll. Soc. Geol. It., 110, 1–8.

D'ARGENIO, B. & MINDSZENTY, A. (1992): Tectonic and climatic control on paleokarst and baxuites.– Giornale di Geologia, 54/1, 207–218.

D'ARGENIO, B. & MINDSZENTY, A. (1995): Bauxites and related paleokarst. Tectonic and climatic event markers at regional unconformities.– Ecl. Geol. Helv., 88/3, 453–499.

DECONINCK, J.F. & STRASSER, A. (1987): Sedimentology, clay mineralogy and depositional environment of Purbeckian green marls (Swiss and Fench Jura).– Eclog. Geol. Helv., 79, 753–772.

DECONINCK, J.F., STRASSER, A. & DEBRABANT, P. (1988): Formation of illitic minerals at surface temperatures in Purbeckian sedimens (Lower Berriasian, Swiss and Ferench Jura).– Clay Miner., 23, 91–103.

DERCOURT, J., ZONENSHAIN, L.P., RICOU, E., KAZMIN, V.G., LE PICHON, X., KNIPPER, A.L., GRANDJACQUET,

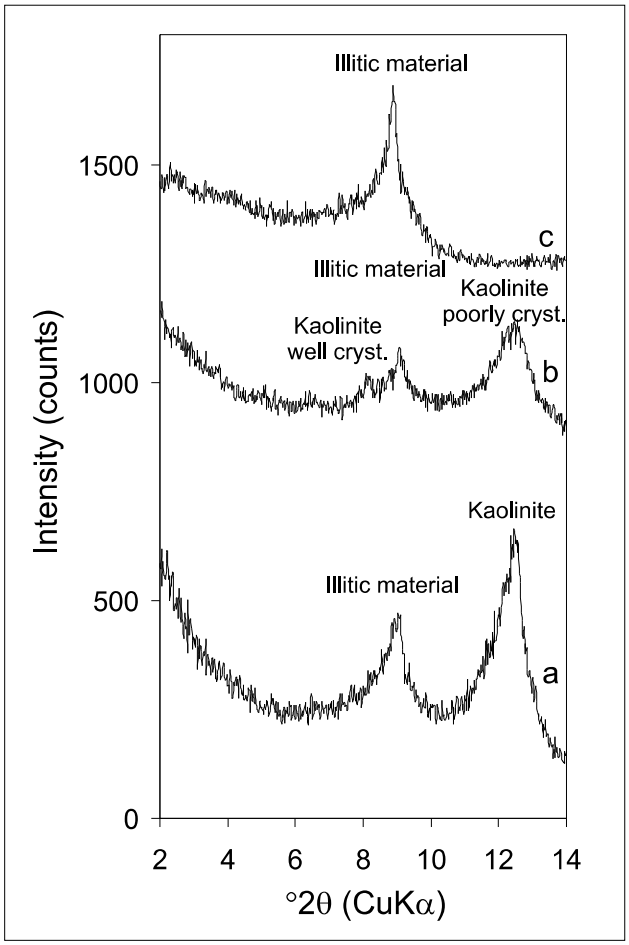

Fig. 37 Characteristic parts of XRD patterns of clay sample 136 (<2 µm fraction): (a) K-saturated; (b) K-saturated and DMSO-solvated; (c) Heated for one hour at 550°C.

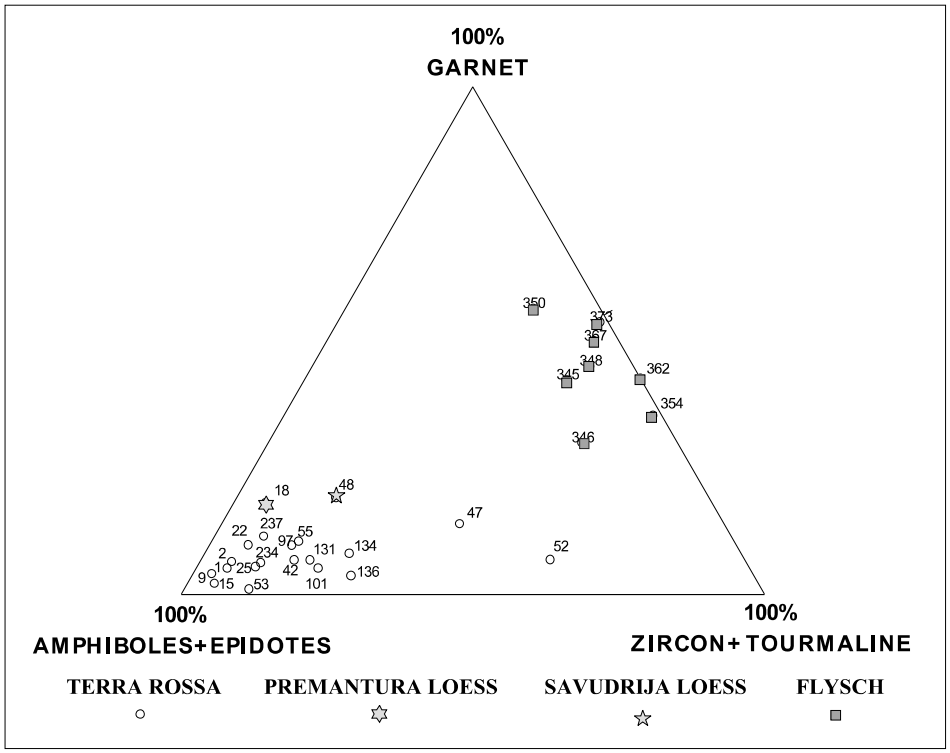

Fig. 38 Relationship between the composition of the selected heavy minerals in *terra rossa*, loess and flysch. Data for *terra rossa* and loess from DURN (1996), data for flysch from MAGDALENIĆ (1972).

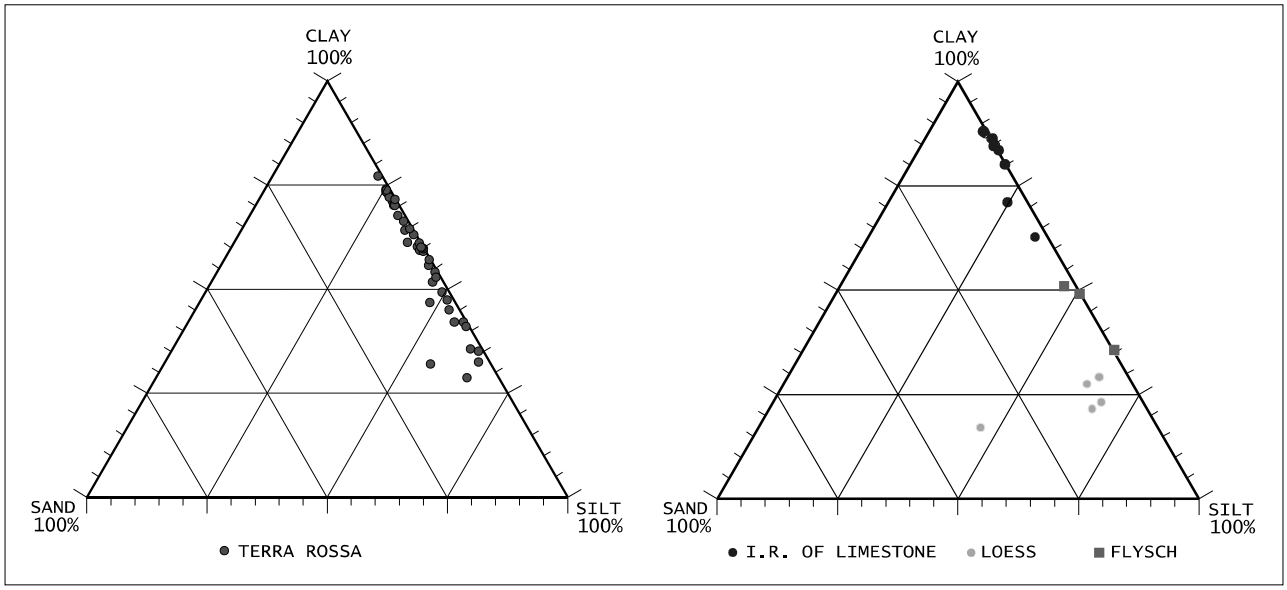

Fig. 39 Particle size analysis of *terra rossa* and insoluble residues of limestone, dolomite, loess and flysch (data from DURN et al., 1999).

C., SBORTSHIKOV, I.M., GEYSSANT, J., LEPVRIER, C., PECHERSKY, D.H., BOULIN, J., SIBUET, J.-C., SAVOSTIN, L.A., SOROKHTIN, O., WESTPHAL, M., BAZHENOV, M.L., LAUER, J.P. & BIJU-DUVAL, B. (1986): Geological evolution of the Tethys belt from the Atlantic to the Pamir since the Lias.– Tectonophysics, 123/1–4, 241–315.

DI STEFANO, P., MALLARINO, G., MINDSZENTY, A. & NICHITTA, D. (2002): Monte Gallo: A Jurassic angular unconformity marked by bauxites in the Panormide carbonate platform.– In: SANTANTONIO, M. (ed.): 6th Intern Symp. on the Jurassic System, Palermo, Italy. General field trip guidebook, 31–35.

DUDICH, E. & MINDSZENTY, A. (1984): Ásvány-kőzettani-geokémiai adatok a Villányi hegység és az Erdélyi Középhegység bauxitjának összehasonlításához (Comparison of the lithology and geochemistry of the Villány and Apuseni bauxites).– Földtani Közlöny (Bull. Geol. Soc. Hung.), 114/1, 1–18, Budapest.

DURN, G. (1996): Origin, composition and genesis of terra rossa in Istria.– Unpubl. PhD Thesis (in Croatian), University of Zagreb, 204 p.

DURN, G., OTTNER, F. & SLOVENEC, D. (1999): Mineralogical and geochemical indicators of the polygenetic nature of terra rossa in Istria, Croatia.– Geoderma, 91, 125–150.

DURN, G., SLOVENEC, D. & ČOVIĆ, M. (2001): Distribution of iron and manganese in terra rossa from Istria and its genetic implications.– Geologia Croatica, 54/1, 27–36.

DURN, G., OTTNER, F., TIŠLJAR, J., MINDSZENTY, A., & BARUDŽIJA, U. (2003): Regional subaerial unconformities

in shallow-marine carbonate sequences of Istria: sedimentology, mineralogy, geochemistry and micromorphology of associated bauxites, palaeosols and pedo-sedimentary complexes.– In: VLAHOVIĆ, I. & TIŠLJAR, J. (eds.): Evolution of Depositional Environments from the Palaeozoic to the Quaternary in the Karst Dinarides and the Pannonian Basin. Field trip guidebook, 22nd IAS Meeting of Sedimentology. 209–255, Zagreb.

DURN, G., ALJINOVIĆ, D., CRNJAKOVIĆ, M. & LUGOVIĆ, B. (2006): Heavy and light mineral fractions indicate polygenesis of extensive terra rossa soils in Istria, Croatia.– In: MANGE, M. & WRIGHT, D. (eds.): Heavy minerals in use. Developments in Sedimentology, Elsevier (in print).

EBERL, D.D., SRODON, J. & NORTHROP, H.R. (1986): Potassium fixation in smectite by wetting and drying.– In: DAVIES J.A. & HAYERS, K.F. (eds.): Geochemical Processes at Mineral Surfaces.– Am. Chem. Soc. Symp. Ser., 323/14, 296–326.

ELLENBERGER, F. (1955): Bauxites métamorphiques dans le Jurassique de la Vanoise, Savoie.– C.R. somm. Soc. Géol. Fr., Paris, 29–32.

FERLA, P. & BOMMARITO, S. (1988): Bauxiti lateritiche mediogiurassiche nei calcari della piattaforma carbonatica panormide di Monte Gallo (Palermo).– Boll. Soc. Geol. It., 107, 579–591.

GRADSTEIN, F.M., AGTERBERG, F.P., OGG, J.G., HARDENBOL, J., VAN VEEN, P., THIERRY, T. & HUANG, Z. (1994): A Mesozoic time scale.– Journal of Geophysical Research, 99, 24051–24074.

GUŠIĆ, I. & JELASKA, V. (1993): Upper Cenomanian–Lower Turonian sea-level rise and consequences on the Adriatic–Dinaric carbonate platform.– Geol. Rundsch., 82/4, 676–686.

HOWER, J., ESLINGER, E., HOWER, M. & PERRY, E. (1976): Mechanism of burial metamorphism of argillaceous sediments. I. Mineralogical and chemical evidence.– Geol. Soc. Am. Bull., 87, 725–537.

JENKYNS, H.C. (1991): Impact of Cretaceous sea level rise and anoxic events on the Mesozoic carbonate platform of Yugoslavia.– Amer. Ass. Petrol. Geol. Bull., 75, 1007–1017.

MAGDALENIĆ, Z. (1972): Sedimentologija flišnih naslaga srednje Istre.– Acta Geol., 7/2, 71–100.

MALEZ, M. (1981): Karst underground in Istria as a place for settling of fossil people (in Croatian).– In: EKL, V. (ed.): Liburnijske teme, 4 119–135, Opatija.

MANATSCHAL, G. & BERNOULLI, D. (1998): Rifting and early evolution of ancient ocean basins: the record of the Mesozoic Tethys and of the Galicia–Newfoundland margins.– Marine Geophysical Researches, 20, 371–381.

MARINČIĆ, S. & MATIČEC, D. (1991): Tektonika i kinematika deformacija na primjeru Istre (Tectonics and kinematic of deformations – an Istrian model).– Geol. vjesnik, 44, 247–268.

MATIČEC, D., VLAHOVIĆ, I., VELIĆ, I. & TIŠLJAR, J. (1996): Eocene limestones overlying Lower Cretaceous deposits of western Istria (Croatia): Did some parts of present Istria form land during the Cretaceous?– Geologia Croatica, 49/l, 117–127.

MINDSZENTY, A. & D'ARGENIO, B. (1994): Carbonate platform emergence and bauxite formation.– AAPG Annual Convention, Abstracts, Denver, 217.

MOLINA, J.M., RUIZ-ORTIZ, P., VERA, J.A. (1991): Jurassic bauxites in the Subbetic, Betic Cordillera, Southern Spain.– In: Tethyan Bauxites IGCP–287 Part–I. Acta Geol. Hung., 34/3, 163–178.

MORESI, M. & MONGELLI, G. (1988): The relation between the terra rossa and the carbonate-free residue of the underlying limestones and dolostones in Apulia, Italy.– Clay Minerals, 23, 439–446.

MUHS, D.R., BUSH, C.A. & STEWART, K.C. (1990): Geochemical evidence of Saharan dustparent material for soils developed on Quaternary limestone of Caribbean and Western Atlantic islands.– Quaternary Research, 33, 157–177.

MUHS, D.R., CRITTENDEN, R.C., ROSHOLT, J.N., BUSH, C.A. & STEWART, K.C. (1987): Genesis of marine terrace soils, Barbados, West Indies: Evidence from mineralogy and geochemistry.– Earth Surface Processes and Landforms, 12, 605–618.

MUNSELL COLOR CHARTS (1994): Munsell Soil Color Charts.– Macbeth Division of Kollmorgem Instruments Corporation, New Windsor.

NICHITTA, D. (1988): Stratigrafia e sedimentologia dei carbonati di piattaforma del Giurassico Superiore–Cretacico nel settore nord–orientale dei Monti di Palermo.– Unpubl. PhD Thesis, University of Palermo, 212 p.

POLŠAK, A. (1970): Osnovna geološka karta SFRJ 1:100.000, Tumač za list Pula L33–112 (Basic Geological Map of SFRY, 1:100000, Geology of the Pula sheet).– Institut za geološka istraživanja, Zagreb, Savezni geološki zavod, Beograd, 44 p.

POLŠAK, A. & ŠIKIĆ, D. (1973): Osnovna geološka karta SFRJ 1:100.000, Tumač za list Rovinj (Basic Geological Map of SFRY, 1:100000, Geology of the Rovinj sheet).– Institut za geološka istraživanja, Zagreb, Savezni geološki zavod, Beograd, 51 p.

RADOJČIĆ, R. (1982): Carbonate platforms of the Dinarids: the example of Montenegro–West Serbia sector.– Bull. T. LXXX, Acad Serbe des Sci. et des Arts, Classe Sci. nat. et math., 22, 35–46, Beograd.

RASMUSSEN, K. & NEUMANN, A.C.N. (1988): Holocene overprint of Pleistocene paleokarst: Bight of Abaco, Bahamas.– In: JAMES, N.P. & CHOQUETTE, P.W. (eds.): Paleokarst. Springer Verlag, 132–148.

ROBINSON, D. & WRIGHT, V.P. (1987): Ordered illite–smectite and kaolinite–smectite: Pedogenic minerals in a Lower Carboniferous paleosol sequence, South Wales.– Clay Miner., 22, 109–118.

SIMONE, L., CARANNANTE, G., D'ARGENIO, B., RUBERTI, D. & MINDSZENTY, A. (1991): Bauxites and related paleokarst in Southern Italy, Sicily and Sardinia.– In: Tethyan Bauxites IGCP–287 Part II. Acta Geol.Hung., 34/4, 273–306.

ŠINKOVEC, B. (1974): Jurski glinoviti boksiti zapadne Istre.– Geol. vjesnik, 27, 217–226.

ŠINKOVEC, B. & SAKAČ, K. (1991): Bauxite deposits of Yugoslavia – the state of the art.– In: Tethyan Bauxites IGCP 287 Part II., Acta Geol. Acad. Sci. Hung., 34/4, 307–316. 315316.

STAMPFLI, G.M. & MOSAR, J. (1999): The making and becoming of Apulia.– In: GOSSO, G., JADOUL, F., SELLA, M. & SPALLA, M.I. (eds.): 3rd Workshop on Alpine Geological Studies. Memorie di scienze Geologiche, 51/1, 141–154, Padova.

TIŠLJAR, J. (1978): Onkolitni i stromatolitni vapnenci u donjokrednim sedimentima Istre (Oncolites and stromatolites in Lower Cretaceous carbonate sediments of Istria (Croatia, Yugoslavia)).– Geološki vjesnik, 30/2, 363–382.

TIŠLJAR, J. (1983): Coated grains facies in the Lower Cretaceous of the Outer Dinarides (Yugoslavia).– In: Peryt, T. (ed.):

Coated Grains. Springer-Verlag, Berlin–Heidelberg–New York–Tokyo, 566–576.

TIŠLJAR, J. (1986): Postanak crnih valutica i oblutaka ("black pebbles") u periplimnim vapnencima titona zapadne Istre i barema otoka Mljeta (Origin of the black-pebbles and fragments in the peritidal limestones of the western Istria (Tithonian) and Island of Mljet (Barremian)).– Geol. vjesnik, 39, 75–94.

TIŠLJAR, J. & VELIĆ, I. (1987): The Kimmeridgian tidal-bar calcarenite facies of Western Istria (Western Croatia, Yugoslavia).– Facies, 17, 277–284.

TIŠLJAR, J. & VELIĆ, I. (1991): Carbonate facies and depositional environments of the Jurassic and Lower Cretaceous of the coastal Dinarides (Croatia).– Geol. vjesnik, 44, 215–234.

TIŠLJAR, J., VELIĆ, I. & VLAHOVIĆ, I. (1994): Facies diversity of the Malmian platform carbonates in Western Croatia as a consequence of synsedimentary tectonics.– Géologie Méditerranéenne, 3–4, 173–176.

TIŠLJAR, J., VLAHOVIĆ, I., MATIČEC, D. & VELIĆ, I. (1995): Platformni facijesi od gornjeg titona do gornjega alba u zapadnoj Istri i prijelaz u tempestitne, klinoformne i rudistne biolititne facijese donjega cenomana u južnoj Istri, ekskurzija B (Platform facies from the Upper Tithonian to Upper Albian in western Istria and transition into tempestite, clinoform and rudist biolithite facies of the Lower Cenomanian in southern Istria).– In: VLAHOVIĆ, I. & VELIĆ, I. (eds.): lst Croatian Geological Congress, Excursion Guide-Book, 67–110, Zagreb.

TIŠLJAR, J., VLAHOVIĆ, I., VELIĆ, I., MATIČEC, D. & ROBSON, J. (1998): Carbonate facies evolution from the Late Albian to Middle Cenomanian in southern Istria (Croatia): influence of synsedimentary tectonics and extensive organic carbonate production.– Facies, 38, 137–152.

TIŠLJAR, J., VLAHOVIĆ, I., VELIĆ, I. & SOKAČ, B. (2002): Carbonate platform megafacies of the Jurassic and Cretaceous deposits of the Karst Dinarides.– Geologia Croatica, 55/2, 139–170.

VANSTONE, S.D. (1988): Late Dinantian paleokarst of England and Wales: implications for exposure surface development.– Sedimentology, 45, 19–37.

VELIĆ, I. & TIŠLJAR, J. (1987): Biostratigrafske i sedimentološke značajke donje krede otoka Veli Brijun i usporedba s odgovarajućim naslagama jugozapadne Istre (Biostratigraphic and sedimentologic characteristics of the Lower Cretaceous deposits of the Veli Brijun island and comparison with the corresponding deposits in SW Istria (western Croatia, Yugoslavia)).– Geol. vjesnik, 40, 149–168.

VELIĆ, I. & TIŠLJAR, J. (1988): Litostratigrafske jedinice u dogeru i malmu zapadne Istre, zapadna Hrvatska, Jugoslavija (Lithostratigraphic units in the Dogger and Malm of western Istria).– Geol. vjesnik, 41, 25–49.

VELIĆ, I., TIŠLJAR, J. & SOKAČ, B. (1989): The variability of thicknesses of the Barremian, Aptian and Albian carbonates as a consequence of changing depositional environments and emersion in Western Istria (Croatia, Yugoslavia).– Mem. Soc. Geol. It., 40 (1987), 209–218.

VELIĆ, I., TIŠLJAR, J., MATIČEC, D. & VLAHOVIĆ, I. (1995a): Opći prikaz geološke grade Istre (A review of the geology of Istria).– In: VLAHOVIĆ, I. & VELIĆ, I. (eds.): lst Croatian Geological Congress, Excursion Guide-Book, 5–30, Zagreb.

VELIĆ, I., MATIČEC, D., VLAHOVIĆ, I. & TIŠLJAR, J. (1995b): Stratigrafski slijed jurskih i donjokrednih karbonata (bat–gornji alb) u zapadnoj Istri (ekskurzija A) (Stratigraphic succession of Jurassic and Lower Cretaceous Carbonates (Bathonian–Upper Albian) in western Istria (Excursion A)).– In: VLAHOVIĆ, I. & VELIĆ, I. (eds.): 1 st Croatian Geological Congress, Excursion GuideBook, 31–66, Zagreb.

VERA, J.A., RUIZ-ORTIZ, P.A., GARCIA HERNANDEZ, M. & MOLINA, J.M. (1988): Paleokarst and related pelagic sediments in the Jurassic of the Subbetic Zone, Southern Spain.– In: JAMES, N.P. & CHOQUETTE, P.W. (eds.): Paleokarst. Springer Verlag, 364–384.

VLAHOVIĆ, I. (1999): Karbonatni facijesi plitkovodnih taložnih sustava od kimeridža do gornjega alba u zapadnoj Istri (Carbonate facies of shallow water depositional systems from Kimmeridgian to the Upper Albian in Western Istria).– Unpubl. PhD Thesis (in Croatian with English summary), University of Zagreb, 327 p.

VLAHOVIĆ, I., TIŠLJAR, J. & VELIĆ, I. (1994): Facies succession in the Cenomanian of Istria (Western Croatia): tectonic vs. eustatic control.– First International Meeeting on Perimediterranean Carbonate Platforms, Abstracts, 169–171, Marseille.

VLAHOVIĆ, I., TIŠLJAR, J., VELIĆ, I. & MATIČEC, D. (2000): Accumuli bauxitici e cicli peritidali shallowing upwards del giurassico superiore.– In: CARULLI, G.B. (ed.): Guida alle escursioni. 80a Riunione Estiva della S.G.I., Trieste, 245–252.

VLAHOVIĆ, I., KORBAR, T., MORO, A., VELIĆ, I., SKELTON, W.P., FUČEK, L. & TIŠLJAR, J. (2002): Latest Cenomanian to Earliest Turonian platform drowning and Turonian recovery of shallow-water platform deposition in southern Istria.– In: VLAHOVIĆ, I. & KORBAR, T. (eds.) Abstracts and Excursion Guidebook – 6th International Congress on Rudists, Rovinj – Croatia. Institut za geološka istraživanja, Zagreb, 123–127.

VLAHOVIĆ, I., TIŠLJAR, J., VELIĆ, I., MATIČEC, D., SKELTON, P.W., KORBAR, T. & FUČEK, L. (2003): Main events recorded in the sedimentary succession of the Adriatic Carbonate Platform from the Oxfordian to the Upper Santonian in Istria (Croatia).– In: VLAHOVIĆ, I. & TIŠLJAR, J. (eds.): Evolution of Depositional Environments from the Palaeozoic to the Quaternary in the Karst Dinarides and the Pannonian Basin. Field Trip Guidebook. 22nd IAS Meeting of Sedimentology, Opatija – September 17–19, 2003, 19–56, Zagreb.

VLAHOVIĆ, I., TIŠLJAR, J., VELIĆ, I. & MATIČEC, D. (2005): Evolution of the Adriatic Carbonate Platform: palaeogeography, main events and depositional dynamics.– Palaeogeography, Palaeoclimatology, Palaeoecology, 220, 333–360.

WINCHESTER, J.A. & FLOYD, P.A. (1977): Geochemical discrimination of different magma series and their differentiation products using immobile elements.– Chemical Geology, 20, 325–343.

YAALON, D.H. (1997): Soils in the Mediterranean region: what makes them different?– Catena, 28, 157–169.